Large Scale Structures and Structure Formation

The Lumpy Universe

So far: treated universe as smooth universe.

In reality:

Universe contains structures!

Last part of this class:

1. What are structures?
2. How can we quantify them?
3. How do structures form?
4. How do structures evolve?

Will see that all these questions are deeply connected with parameters of the universe seen so far:

1. H_0
2. Ω_0, Ω_b, Ω_m, Ω_Λ,...
3. Existence and Nature of Dark Matter

Introduction

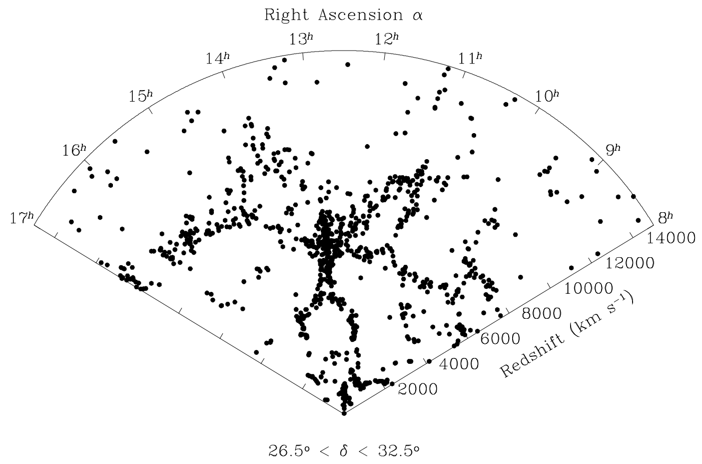

(de Lapparent et al., 1986, limiting mag $m_B = 15.6$)

Lumpy universe: spatial distribution of galaxies and greater structures.

Introduction

How do we study the structure of the Universe?

$\Longrightarrow$ We need distance information for many ($10^4 \dots 10^7$) objects

$\Longrightarrow$ Large redshift surveys

Review: Strauss & Willick (1995)

Redshift survey: Survey of (patch of) sky determining galaxy z and position to predefined magnitude or z.

First larger survey: de Lapparent et al. (1986)

Classification:

1D-surveys: very deep exposures of small patch of sky, e.g., HST Deep Field, Lockman Hole Survey, COSMOS Field, Marano Field.

2D-surveys: cover long strip of sky, e.g., CfA-Survey ($1.5 \times 100°$), 2dF-Survey ("2 degree Field").

3D-surveys: cover part of the sky, e.g., Sloan Digital Sky Survey.

These surveys attempt to go to certain limit in z or m.

Other approaches: use pre-existing galaxy catalogues (e.g., QDOT Survey [IRAS galaxies], APM survey,...).

We will concentrate here on the larger surveys based on no other catalogue.

Introduction

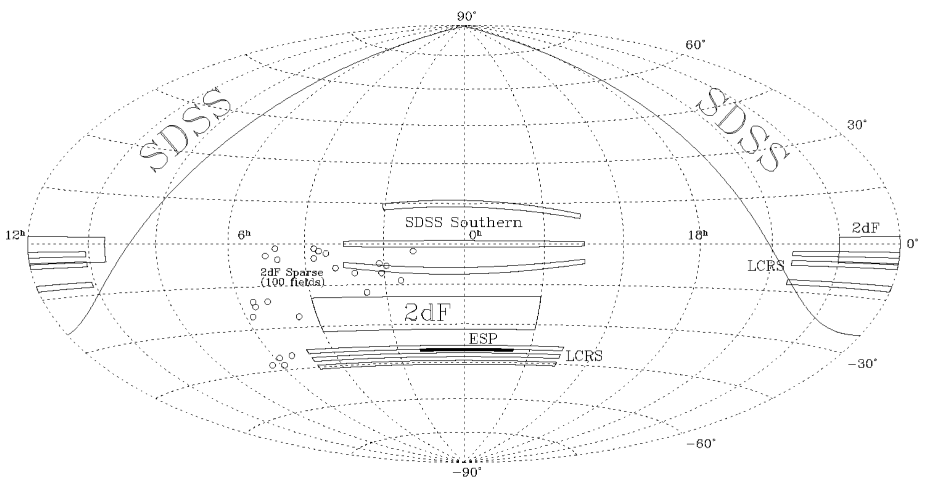

(Strauss, 1999)

Ground: Subaru (8m) Space: *HST* (2.4m)

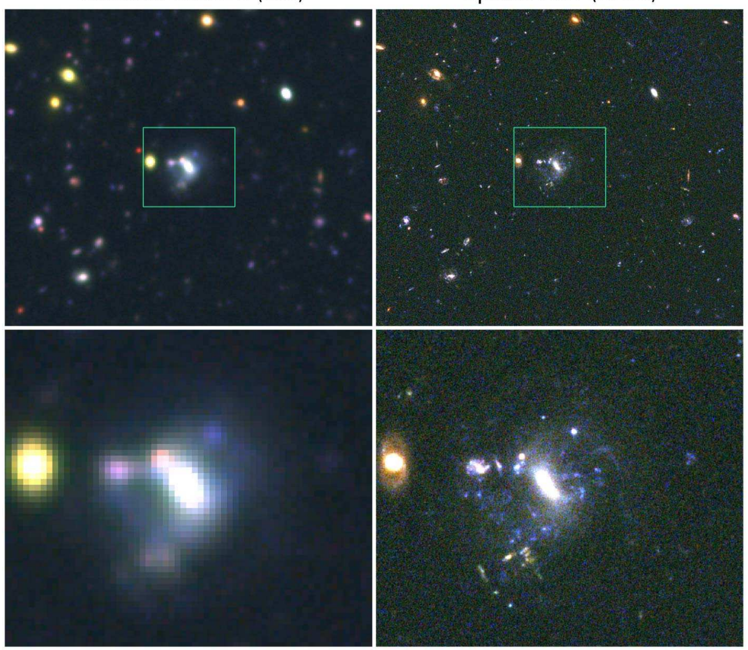

To go deep one needs to go to space

STScI

Hubble Space Telescope

The Hubble Space Telescope has a large set of instruments well suited for cosmological observations:

Current HST Instruments :

- WFC3: Wide Field Camera 3 (05.2009–)
- COS: Cosmic Origins Spectrograph (05.2009–)
- ACS: Advanced Camera for Surveys (03.2002–)
- STIS: Space Telescope Imaging Spectrograph (02.1997–)
- NICMOS: Near Infrared Camera and Multi Object Spectrometer (02.1997–)
- FGS: Fine Guidance Sensors

Former Generation Instruments :

- FOC: The Faint Object Camera (04.1990–03.2002)
- FOS: The Faint Object Spectrograph (04.1990–02.1997)
- GHRS: The Goddard High Resolution Spectrograph (04.1990–02.1997)
- HSP: The High Speed Photometer (04.1990–10.1993)
- WF/PC-1: Wide Field Planetary Camera 1 (04.1990–10.1993)
- WFPC2 The Wide Field Planetary Camera 2 (12.1993–05.2009)

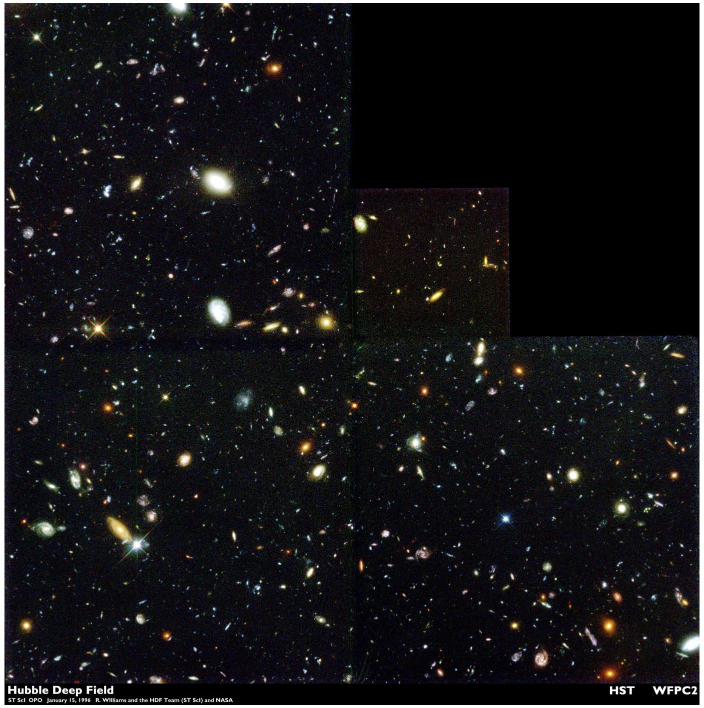

1995 December: Hubble Deep Field: $\sim$ 150 ksec/Filter for four HST Filters

Many galaxies with weird shapes $\Longrightarrow$ protogalaxies!

Redshifts: $z \in [0.5, 5.3]$ (Fernández-Soto et al., 1999)

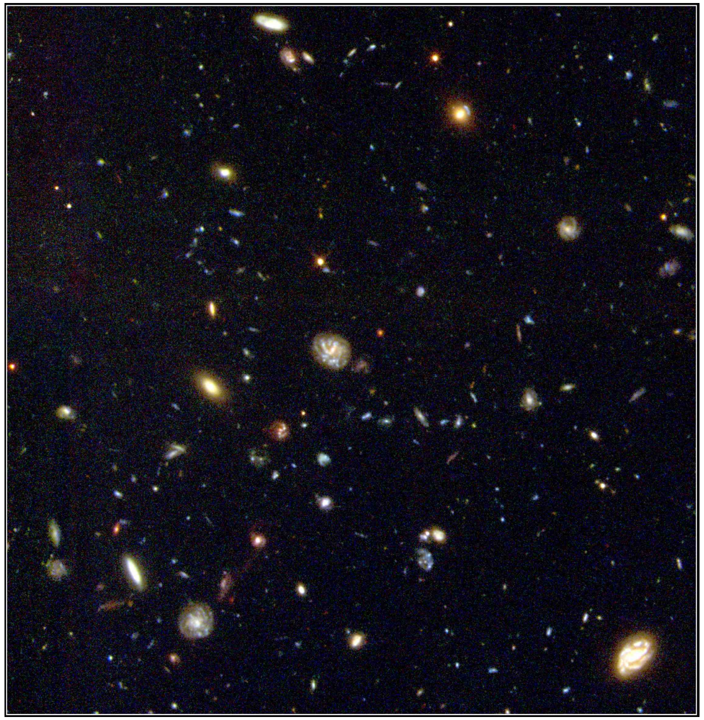

1998: Hubble Deep Field South, 10 d of total observing time!

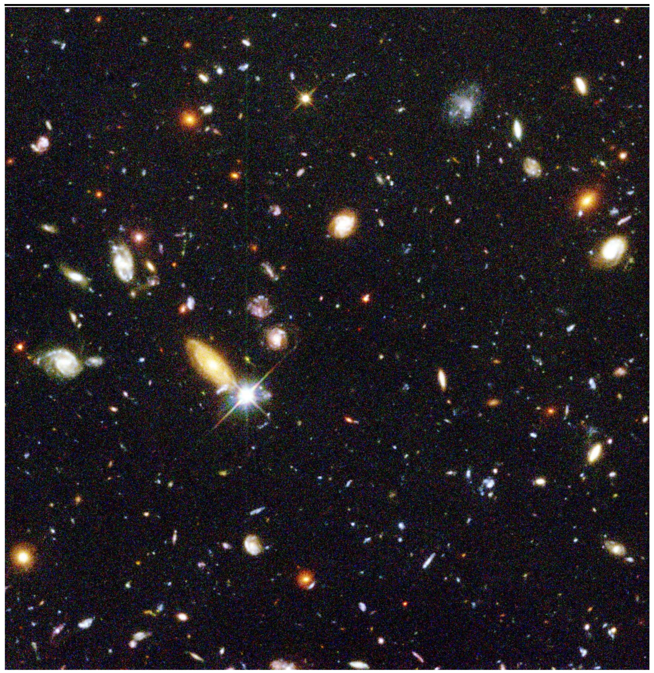

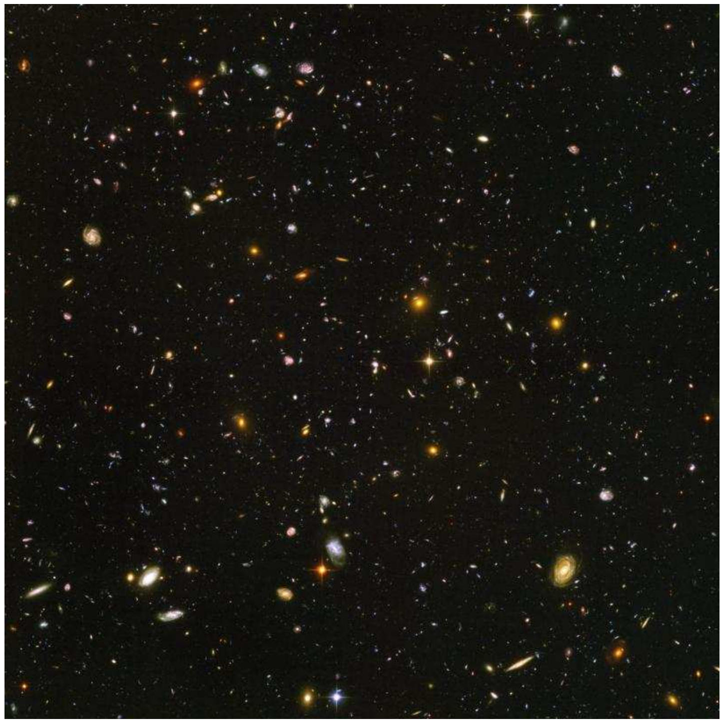

2004: Hubble Ultra Deep Field, 1 Msec long exposure of field in Fornax. Uses updated HST with Advanced Camera for Surveys (ACS) and Near Infrared Camera and Multi-Object Spectrometer (NICMOS); diameter: $3'$ ($2\times$ HDF)

Limiting magnitude: 30 mag, $\sim$10000 galaxies visible, up to $z \gtrsim 7$

IR reveals many reddened objects

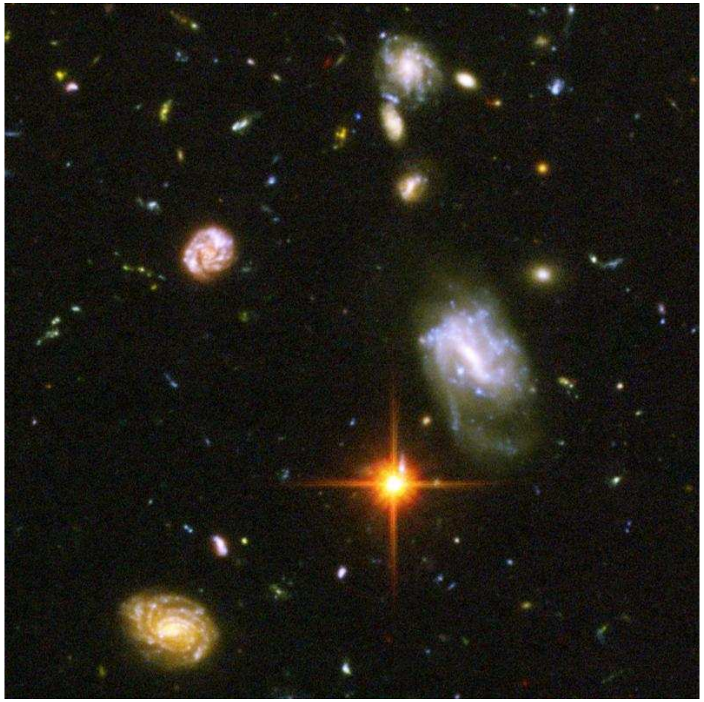

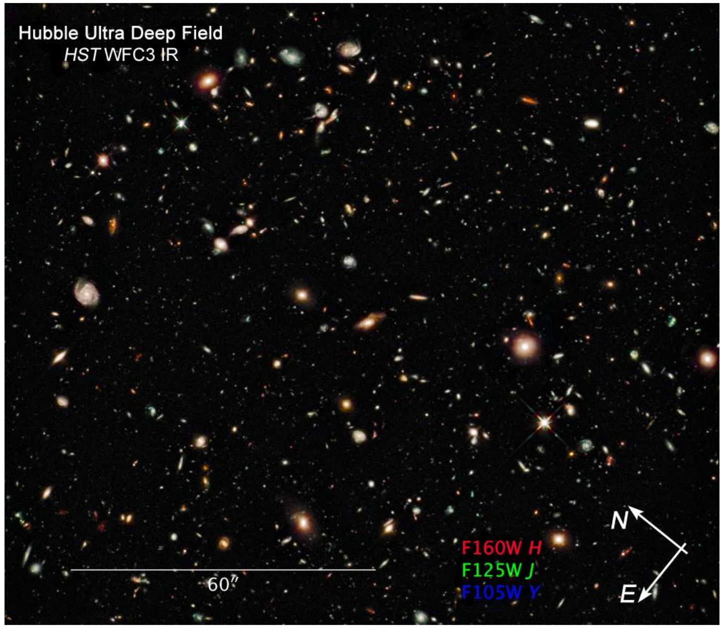

2009 August 26 – 2009 September 2009: WFC3 pushes HUDF even deeper (data taken in same region as HUDF, "Hubble Ultra Deep Field Infrared"). Exposure: 48 h

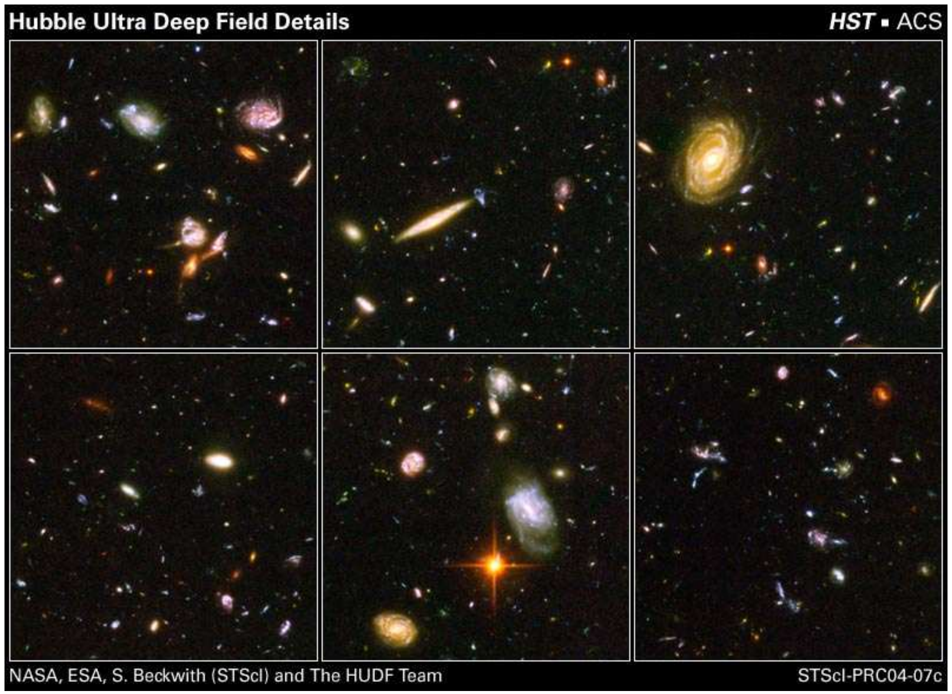

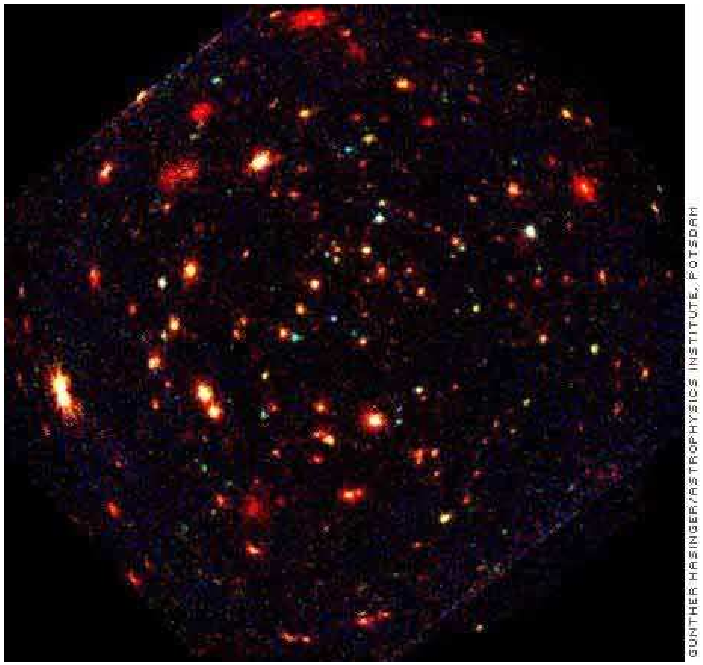

Lockman Hole: Northern Sky region with very low N_{H}

$\Longrightarrow$ low interstellar absorption

$\Longrightarrow$ "Window in the sky"

$\Longrightarrow$ X-rays: evolution of active galaxies with z!

XMM-Newton, Hasinger et al., 2001,
blue: hard X-ray spectrum,
red: soft X-ray spectrum

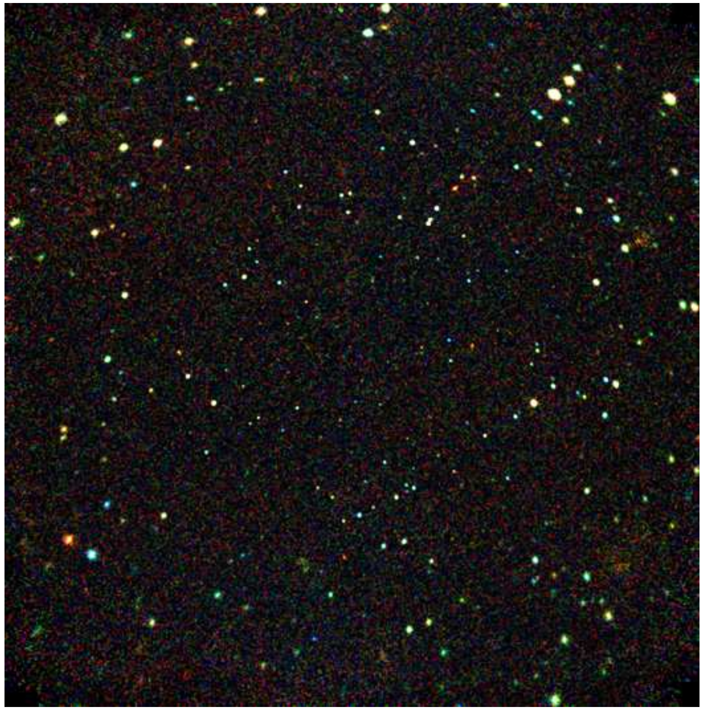

Chandra Deep Field South:
1 Msec (10.8 days) on one region in Fornax ($\alpha_{J2000.0} = 3^h32^m28.0^s$, $\delta_{J2000.0} = -27°48'30''$, coaligned with HDF-S
Deepest X-ray field ever
color code: spectral hardness

scale: $15' \times 15'$; courtesy NASA/JHU/AUI/R.Giacconi et al.

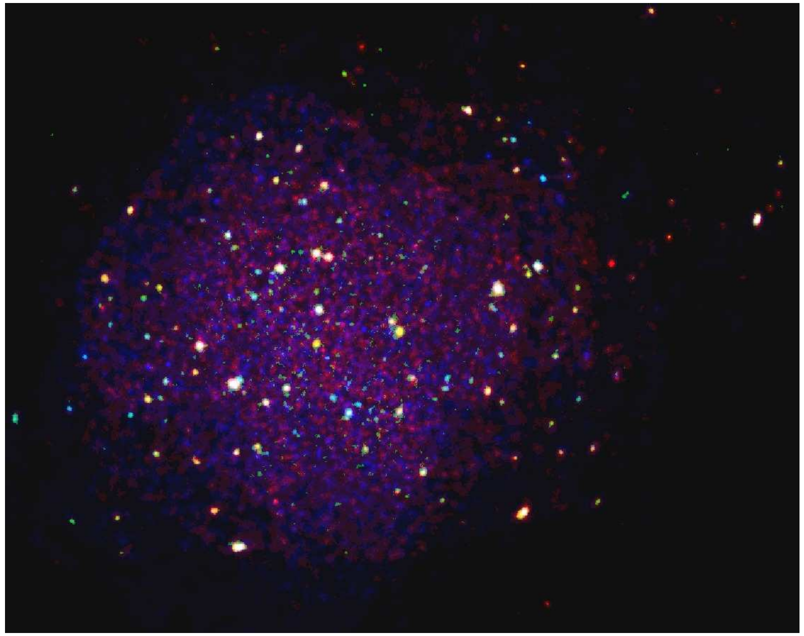

Deep *XMM-Newton* image of the Marano Field (IAAT/AIP/MPE)

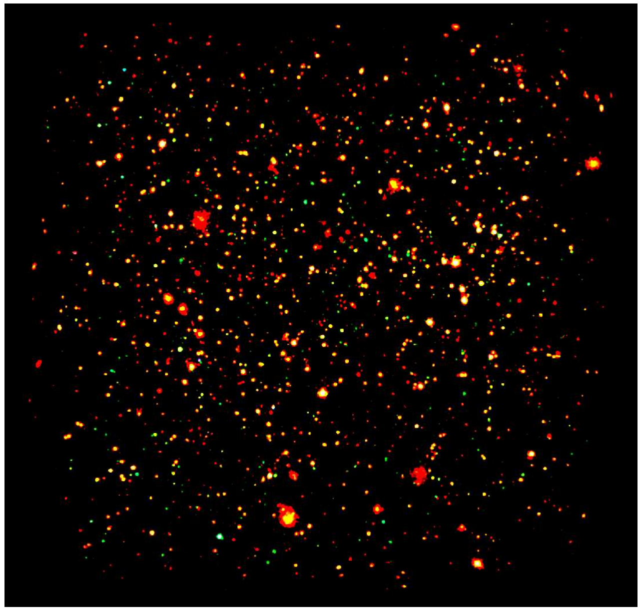

COSMOS-field: large X-ray survey for Galaxy Clusters

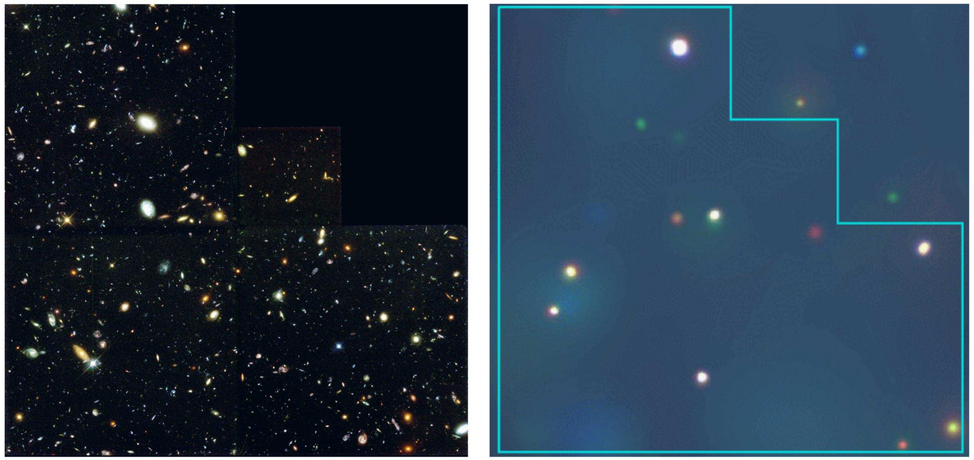

HST Chandra

Chandra/HST Image of Hubble Deep Field North; 500 ksec

Joint multi-wavelength campaigns allow the measurement of broad-band spectra of sources in the early universe!

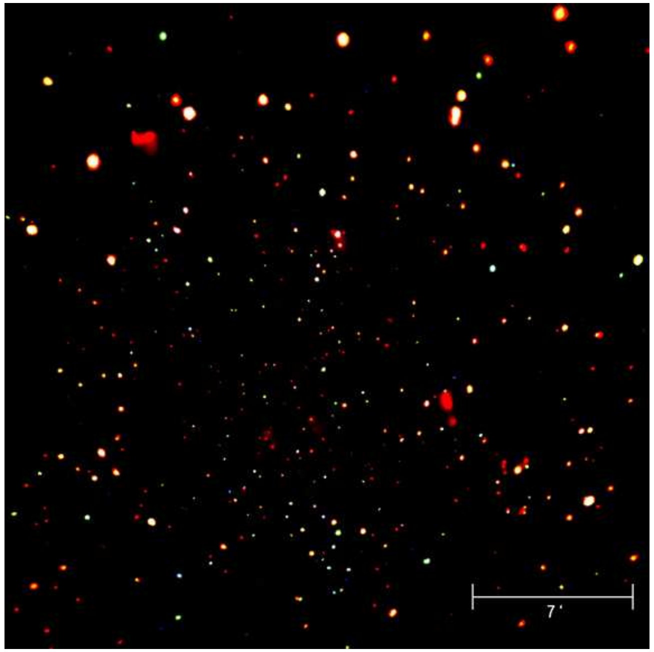

⟹ GOODS-Survey (Great Observatories Origins Deep Survey), centered on CDF-S
(same image as before, this time smoothed)

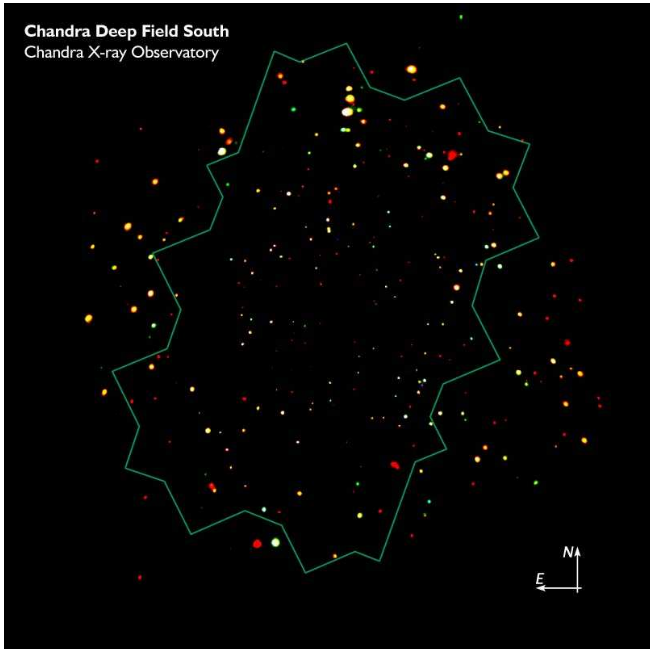

Chandra and HST fields aligned

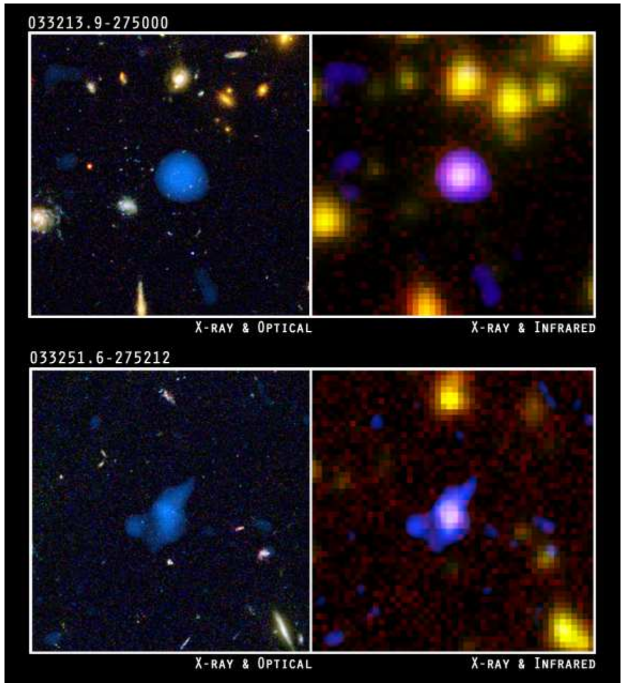

IR, optical, and X-ray image of small fraction of GOODS

CXC/NASA

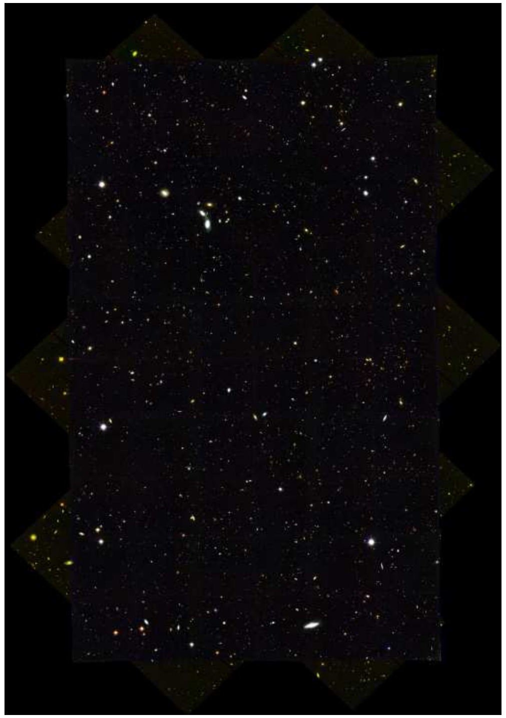

HST ACS observations of whole area of CDF-S

CXC

2D/3D Surveys: Technology

Future for Large Scale Structure: 2D and 3D Surveys observing large part of sky with dedicated instruments.

Currently largest surveys:

Las Campanas Redshift Survey (LCRS): 26418 redshifts in six $1.5 \times 80^\circ$ slices around NGP and SGP, out to $z = 0.2$.

CfA Redshift Survey: 30000 galaxies

APM: (Oxford University) $2 \sim 10^6$ galaxies, 10^7 stars around SGP, 10% of sky, through $B = 21$ mag.

2MASS: IR Survey of complete sky (Mt. Hopkins/CTIO) completed 2000 October 25), 3 bands, $\sim 2 \times 10^6$ galaxies, accompanying redshift survey (8dF, CfA)

Sloan Digital Sky Survey (SDSS): dedicated 2000 October 5, Apache Point Obs., NM, 25% of whole sky, $\sim 10^8$ objects, now in Google Earth

And many more (e.g., Keck, ESO, LSST,...).

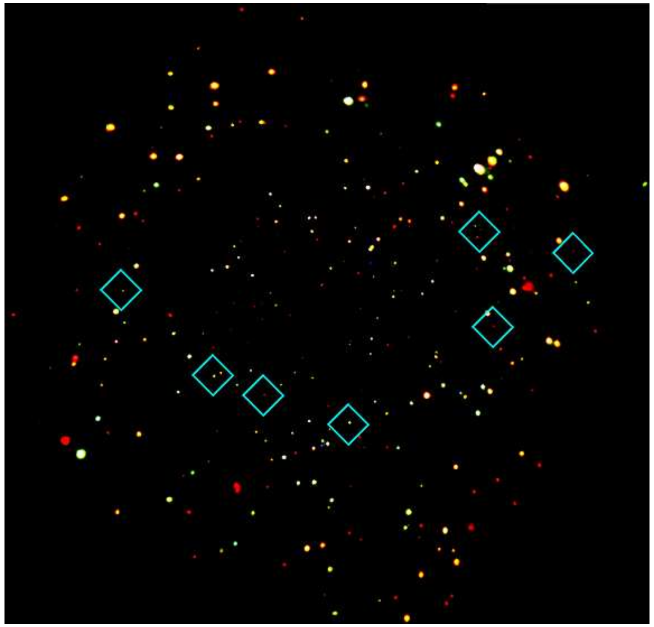

CDFS: blue boxes contain objects not visible in HST
$\Longrightarrow$ farthest black holes known

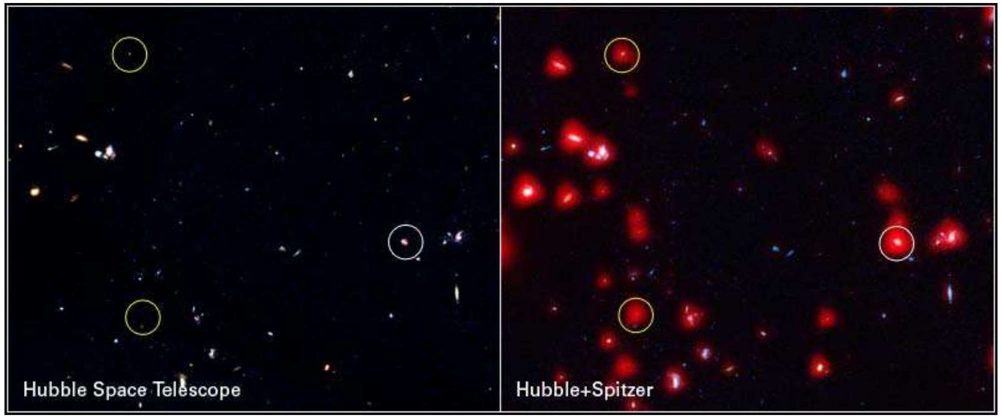

STScI/Caltech

1/200th of the whole GOODS field in optical and IR

SDSS 2.5 m telescope at Apache Point Observatory

courtesy SDSS

2D/3D Surveys: Technology

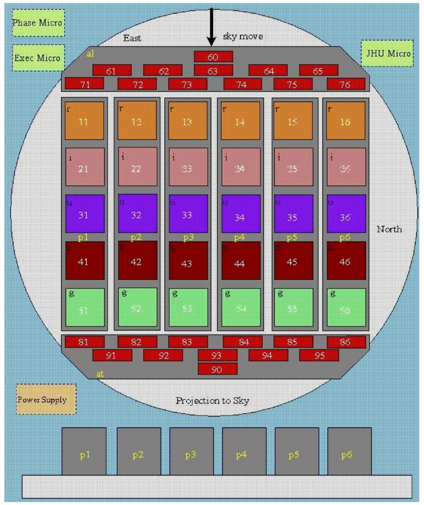

CCD alignment of SDSS:

- focal plane: 2.5°,
- 5 rows of 2048 × 2048 CCDs with r, i, u, z, g filters, saturation at $r = 14$
- 22 2048 × 400 CCD, saturation at $r = 6.6$ for astrometry

Imaging by slewing over CCD Array

SDSS

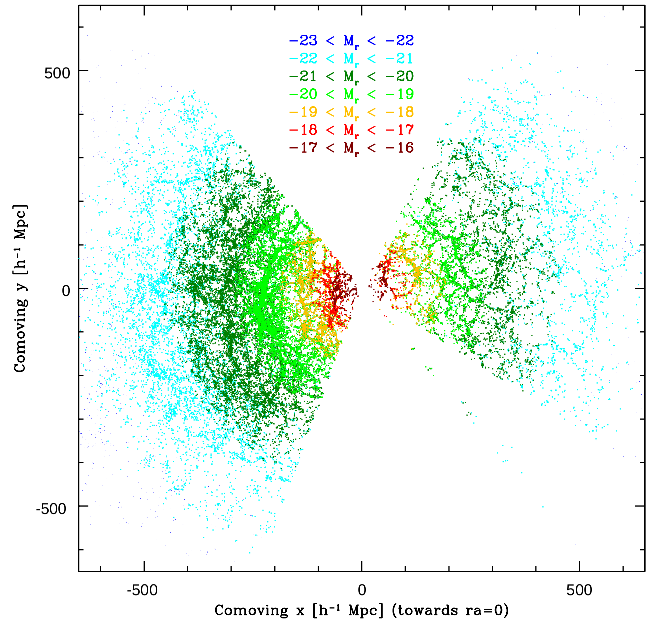

Galaxy distribution from the SDSS

(Tegmark et al., 2004, Fig. 4)

2D/3D Surveys: Technology

courtesy SDSS

Spectroscopy with grism (combination of prism and grating), light from objects via optical fibers and plug plate.

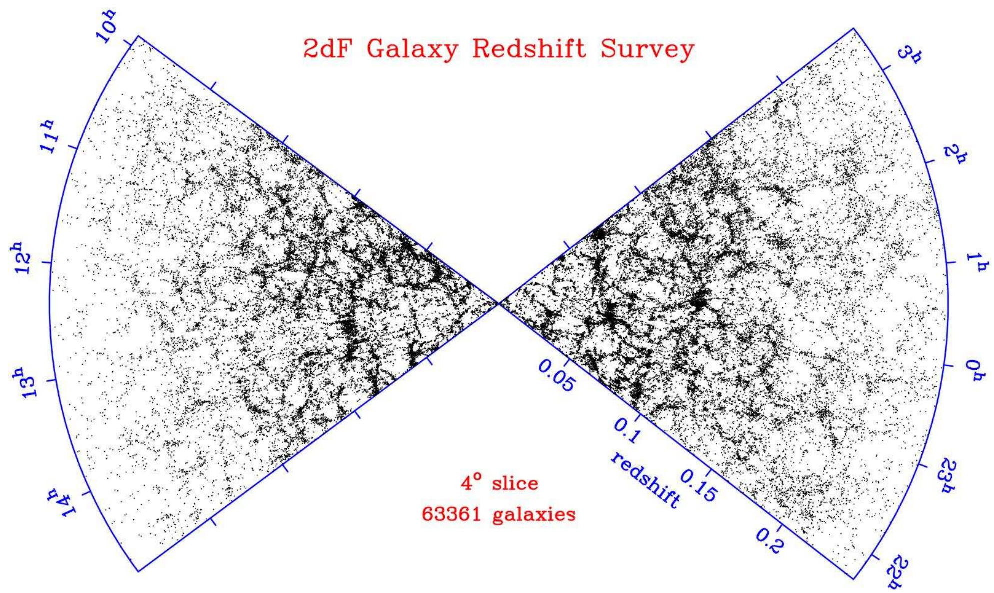

courtesy 2dF collaboration

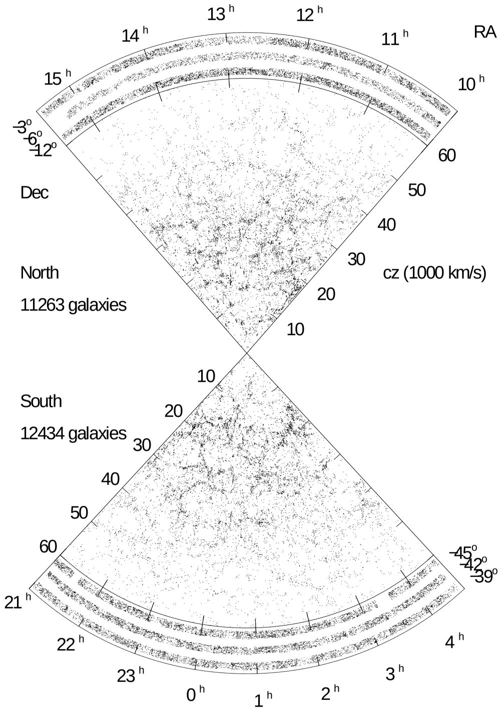

The complete LCRS survey (at cz large: reach mag. limit)

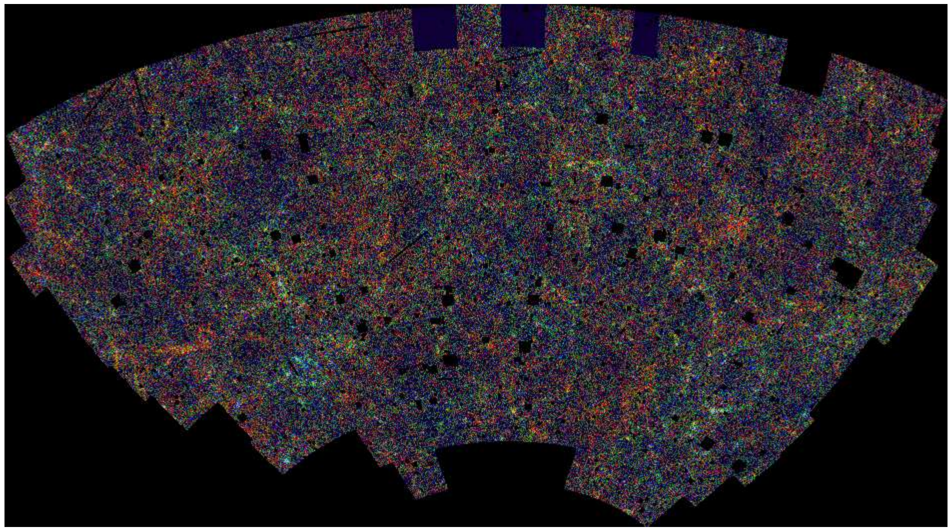

Galaxies in APM catalogue, color: avg. B in pixel: blue (18) – green (19) – red (20)

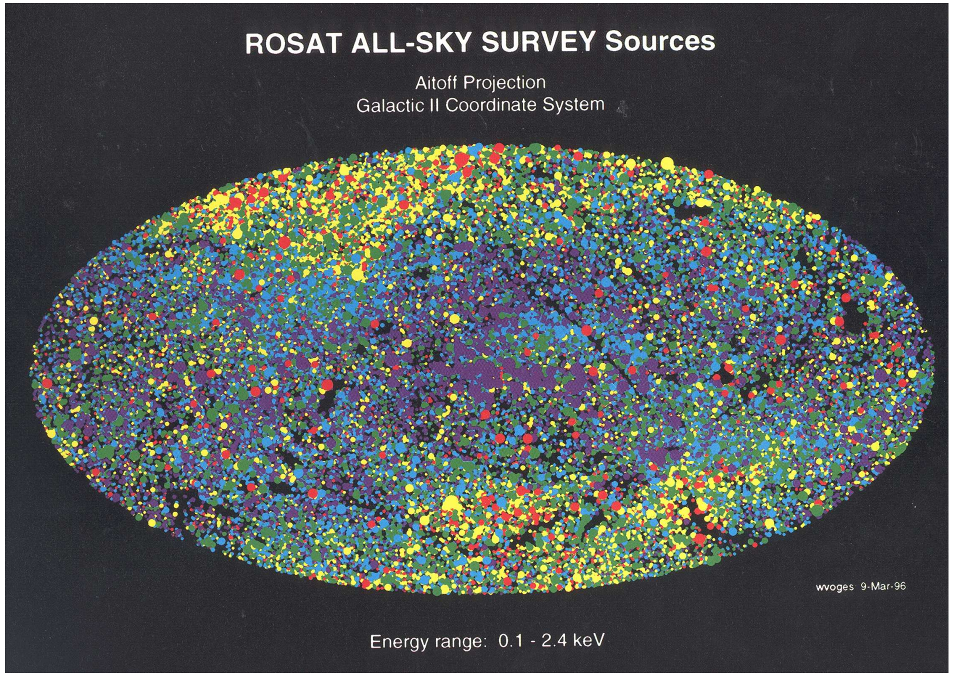

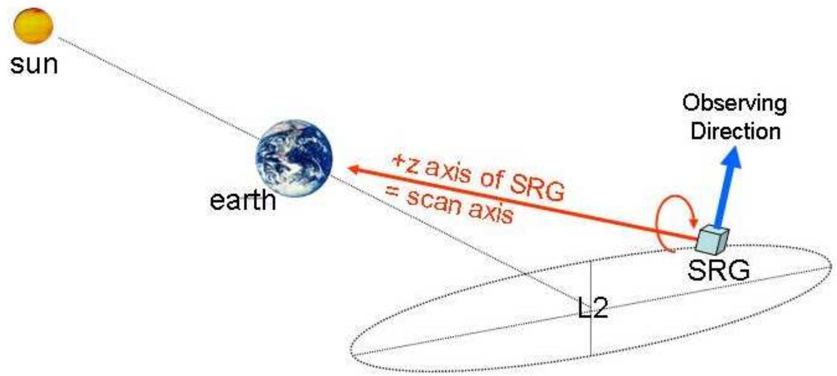

eROSITA (extended ROentgen Survey with an Imaging Telescope Array) on Spectrum-XG

- Launch: Nov 2014, 4 year survey + pointed phase.
- Collaboration: Germany (MPE, IAAT, AIP, FAU, Hamburg)+Russia
- Extends *ROSAT* survey to 10 keV, 30$\times$ deeper
- 3 000 000 supermassive black holes
- 100 000 galaxy clusters $\Longrightarrow \Lambda$, w

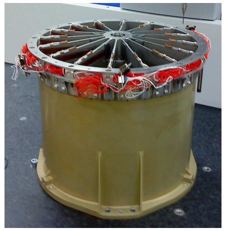

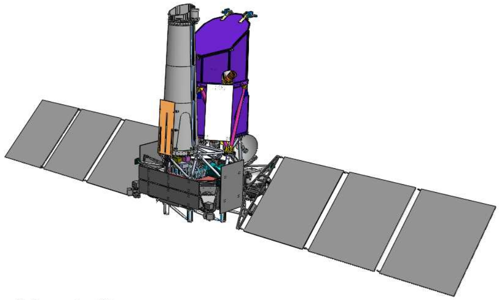

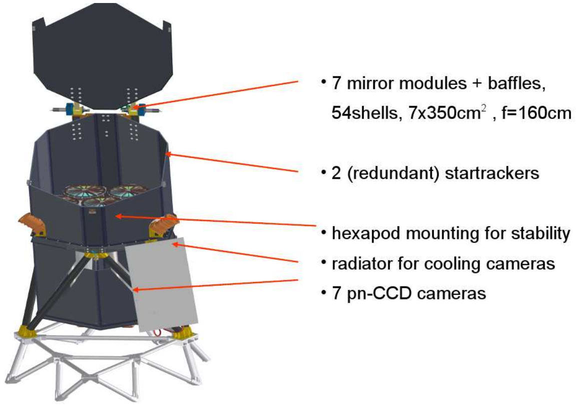

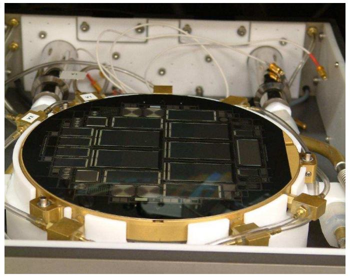

Correlation Function

Sky surveys show:

Galaxies are *not* evenly distributed: "cosmic web"!

- Structures at scales up to several 10 Mpc
- But: Over-density even in clusters not too dramatic ($\sim$ 100$\times$ denser than average)
- Voids on scales 50 h^{-1} Mpc

$\Longrightarrow$ Need quantitative description of structures.

$\Longrightarrow$ Need physical explanation of structures.

$\Longrightarrow$ Need to understand what we see (do galaxies trace matter distribution??).

Correlation Function

Mathematical description of clustering: Correlation function!

Assume *uniform* distribution of galaxies with galaxy density n galaxies Mpc^{-3}.

Probability to find galaxy in volume ΔV:

$$P \propto n\Delta V \tag{14.1}$$

Probability to find galaxies in *two* volumes 1 and 2:

$$P = P_1 \cdot P_2 \propto n^2\,\Delta V_1\,\Delta V_2 \tag{14.2}$$

Universe inhomogeneous: measure (distance dependent) deviation from mean:

$$P \propto n^2(1 + \xi(r_{12}))\,\Delta V_1\,\Delta V_2 \tag{14.3}$$

$\xi(r_{12})$ is called the two-point spatial correlation function.

For *small* r:

$$\xi(r) > 0 \Longrightarrow \text{clustering}$$

Correlation Function

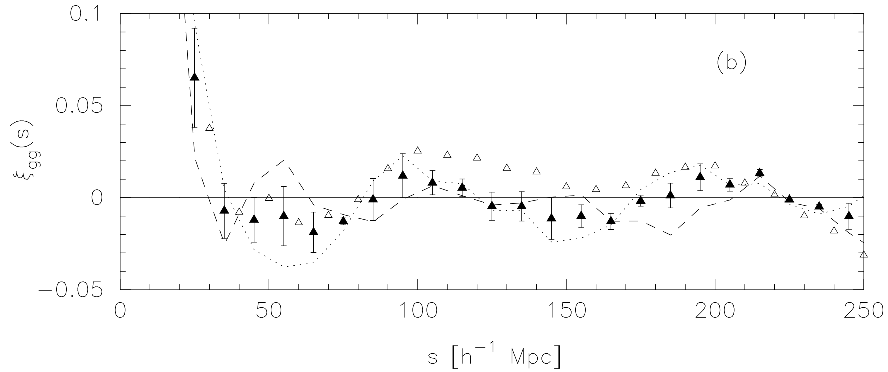

(galaxy-galaxy correlation function from the Las Campanas Redshift Survey; Tucker et al., 1997, Fig. 1)

Rough description: power law

$$\xi(r) = (r/r_0)^{-\gamma} \tag{14.4}$$

where $r_0 \sim 6\,h^{-1}$ Mpc (correlation length), and $\gamma \sim 1.5 \ldots 1.8$.

Above $r = 30\,h^{-1}$ Mpc: oscillation due to voids.

Correlation Function

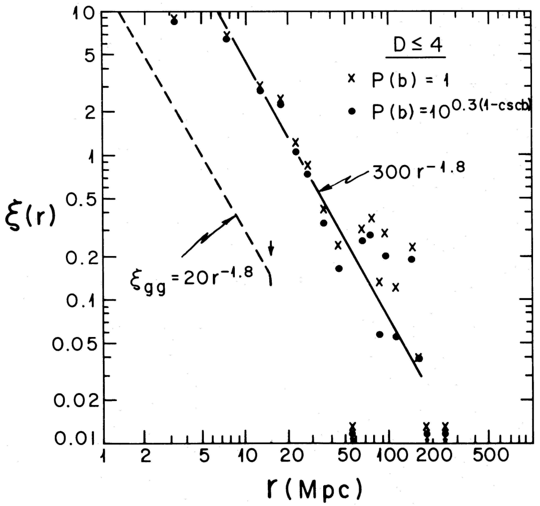

The spatial correlation function for rich (Abell) galaxy clusters is similar to the one for galaxies,

$$\xi_{\text{clusters}}(r) = 360(rh)^{-1.8} \tag{14.5}$$

for $r \leq 150h^{-1}$ Mpc.
For $r > 150h^{-1}$ Mpc no correlations are observed.
Note that richer clusters show stronger correlations.

(Bahcall & Soneira, 1983, Fig. 9a)

Correlation Function

ξ is related to the density contrast $\Delta(x)$:

Write the density n as

$$n(\mathbf{x}) = n_0(1+\Delta(\mathbf{x})) \quad\Longleftrightarrow\quad \Delta(\mathbf{x}) = \delta n/n \tag{14.6}$$

Average joint probability to have galaxies at $\mathbf{x}$ and $\mathbf{x}+\mathbf{r}$:

$$P = \langle n(\mathbf{x})\mathrm{d}V_1 \cdot n(\mathbf{x}+\mathbf{r})\mathrm{d}V_2\rangle \tag{14.7}$$

$$= \left\langle n_0^2(1+\Delta(\mathbf{x}))(1+\Delta(\mathbf{x}+\mathbf{r}))\ \mathrm{d}V_1\mathrm{d}V_2\right\rangle \tag{14.8}$$

Since $\langle\Delta\rangle = 0$, only the cross product survives the averaging:

$$= n_0^2\left(1+\langle\Delta(\mathbf{x})\Delta(\mathbf{x}+\mathbf{r})\rangle\right)\ \mathrm{d}V_1\mathrm{d}V_2 \tag{14.9}$$

where $\langle\ldots\rangle$ denotes averaging over an appropriate volume, i.e.,

$$\langle f(\mathbf{r})\rangle = \frac{1}{V}\int_V f(\mathbf{r})\,\mathrm{d}^3r \tag{14.10}$$

Correlation Function

The two-point correlation function was defined via

$$P \propto n^2(1+\xi(r_{12}))\Delta V_1\Delta V_2 \tag{14.3}$$

while we just found

$$P = n_0^2\left(1+\langle\Delta(\mathbf{x})\Delta(\mathbf{x}+\mathbf{r})\rangle\right)\ \mathrm{d}V_1\mathrm{d}V_2 \tag{14.9}$$

Comparing these two equations shows:

$$\xi(r) = \langle\Delta(\mathbf{x})\Delta(\mathbf{x}+\mathbf{r})\rangle \tag{14.11}$$

$\xi(r)$ is a measure for the average density contrast variations on scales of r.

Power Spectrum

To describe the strength of fluctuations, a good measure is the variance of the density fluctuations.

Let's calculate this around an arbitrary location, $\mathbf{x} = 0$.

$$\text{Var}(n) = \frac{1}{V}\int (n(\mathbf{r}) - \langle n\rangle)^2\,dV \tag{14.12}$$

$$= \frac{1}{V}\int (n_0(1+\Delta(\mathbf{r})) - n_0)^2\,dV \tag{14.13}$$

$$= \frac{n_0^2}{V}\int \Delta(\mathbf{r})^2 dV \tag{14.14}$$

Usually, quantities are normalized to n_0, i.e., relative to mean density $\Longrightarrow n_0 = 1$.

To evaluate the integral, it is more convenient for most calculations to work in Fourier space than in “normal” space.

Define the Fourier transform in spatial coordinates through:

$$\Delta_r(\mathbf{r}) = \frac{V}{(2\pi)^3}\int \Delta_k(\mathbf{k})\exp(-i\mathbf{k}\cdot\mathbf{r})\,\mathrm{d}^3k \tag{14.15}$$

$$\Delta_k(\mathbf{k}) = \frac{1}{V}\int \Delta_r(\mathbf{r})\exp(+i\mathbf{k}\cdot\mathbf{r})\,\mathrm{d}^3r \tag{14.16}$$

Power Spectrum

Therefore

$$\mathrm{Var}(n) = \frac{1}{V}\int \Delta_r(\mathbf{r})^2 \mathrm{d}^3V \tag{14.17}$$
$$= \frac{1}{V}\int \left(\frac{V}{(2\pi)^3}\int \Delta_k \exp(-i\mathbf{k}\cdot\mathbf{r})\,\mathrm{d}^3k\right)^2 \mathrm{d}^3V \tag{14.18}$$
$$= \frac{V}{(2\pi)^6}\int \left(\int \Delta_k \exp(-i\mathbf{k}\cdot\mathbf{r})\,\mathrm{d}^3k\right)\left(\int \Delta_{k'} \exp(-i\mathbf{k}'\cdot\mathbf{r})\,\mathrm{d}^3k'\right) \mathrm{d}^3V \tag{14.19}$$
$$= \frac{V}{(2\pi)^6}\int\int\int \Delta_k\Delta_{k'} \exp\left(-i(\mathbf{k}-\mathbf{k}')\cdot\mathbf{r}\right) \mathrm{d}^3k\,\mathrm{d}^3k'\,\mathrm{d}^3V \tag{14.20}$$
$$= \frac{V}{(2\pi)^6}\int\int \Delta_k\Delta_{k'}(2\pi)^3\delta(\mathbf{k}-\mathbf{k}')\,\mathrm{d}^3k'\mathrm{d}^3k \tag{14.21}$$
$$= \frac{V}{(2\pi)^3}\int \Delta_k^2 \mathrm{d}^3k \tag{14.22}$$

This result is called Parseval's theorem

$$\frac{1}{V}\int \Delta_r^2(\mathbf{r})\,\mathrm{d}^3x = \frac{V}{(2\pi)^3}\int \Delta_k^2(\mathbf{k})\,\mathrm{d}^3k \tag{14.23}$$

(from signal theory: the power in a time series is the same as the power in the associated Fourier transform)

Power Spectrum

Therefore

$$\mathrm{Var}(n) = \langle\Delta^2\rangle = \frac{V}{(2\pi)^3}\int \Delta_k^2 \mathrm{d}^3k = \frac{V}{(2\pi)^3}\int P(k)\,\mathrm{d}^3k \tag{14.24}$$

where the power spectrum is defined by

$$P(k) = \Delta_k^2 = \left(\frac{1}{V}\int \Delta(\mathbf{r})\exp(+i\mathbf{k}\cdot\mathbf{r})\,\mathrm{d}^3r\right)^2 \tag{14.25}$$

The power spectrum is a measure for the strength of density fluctuations at wave number k.

Power Spectrum

How are $P(k) = \langle\Delta^2\rangle$ and ξ related?

$\Longrightarrow$ Use brute force computation or make use of the correlation theorem.

For functions g, h, the correlation theorem states that the Fourier transform of the correlation,

$$\mathrm{Corr}(g,h) = \int g(x+r)h(r)\,\mathrm{d}x \tag{14.26}$$

is given by

$$\mathrm{FT}\left(\mathrm{Corr}(g,h)\right) = G\,H^* \tag{14.27}$$

where $G = \mathrm{FT}(g)$, etc.

Therefore, setting $g = \Delta(r)$ and $h = \Delta(r)$,

$$\xi(r) = \langle\Delta(\mathbf{x})\Delta(\mathbf{x}+\mathbf{r})\rangle = \frac{V}{(2\pi)^3}\int |\Delta_k|^2 \exp(i\,\mathbf{k}\cdot\mathbf{r})\,\mathrm{d}^3k \tag{14.28}$$

The power spectrum and ξ are Fourier transform pairs.

(remember Eq. 14.25, $P(k) = \Delta_k^2$!)

See Peebles (1980, sect. 31) for 100s of pages of the properties of ξ, P, etc.

Power Spectrum: Measurements

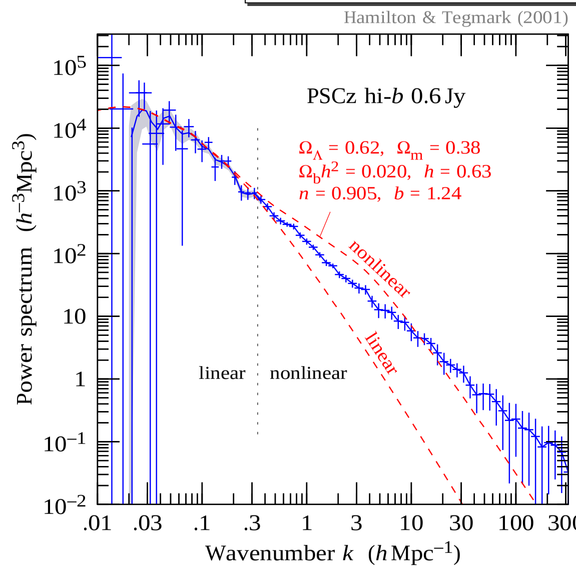

The power spectrum of high galactic latitude IR galaxies is a power-law, roughly described by

$$P(k) \sim 150 k^{-1.46} h^{-3}\,\mathrm{Mpc}^3 \tag{14.29}$$

As we will see later, this result gives problems with results of theory of structure formation, see dashed lines in Figure.

(Hamilton & Tegmark, 2002, Fig. 6)

Power Spectrum: Measurements

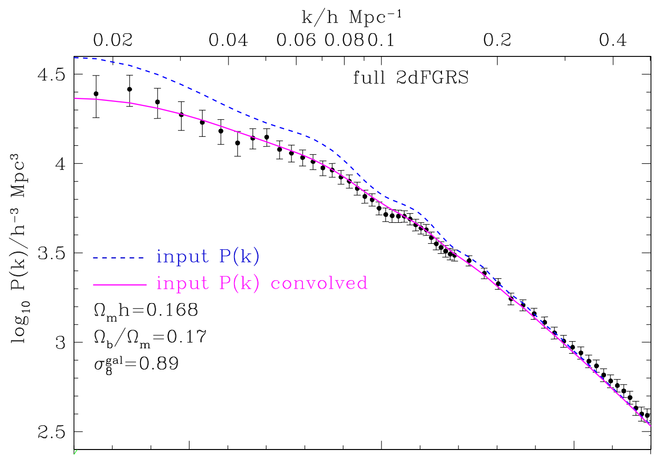

(Cole et al., 2005, Fig. 12)

The galaxy-galaxy-power spectrum flattens towards small k.

Power Spectrum: Interpretation

To understand ξ and P better, let's assume an isotropic universe...

$$\xi(\mathbf{r}) \propto \int P(\mathbf{k}) \exp(i\,\mathbf{k}\cdot\mathbf{r})\,\mathrm{d}^3k \qquad (14.28)$$

Using spherical coordinates in k space, one finds:

$$\mathbf{k}\cdot\mathbf{r} = kr\cos\theta \qquad (14.30)$$

$$\mathrm{d}V = k^2 \sin\theta\,\mathrm{d}\theta\,\mathrm{d}\phi\,\mathrm{d}k \qquad (14.31)$$

such that

$$\xi(r) \propto \int_0^\infty \int_0^\pi \int_0^{2\pi} P(k)\exp(ikr\cos\theta)k^2\sin\theta\,\mathrm{d}\phi\,\mathrm{d}\theta\,\mathrm{d}k \qquad (14.32)$$

$$= 2\pi \int_0^\infty \int_0^\pi P(k)\,\exp(ikr\cos\theta)\,k^2\,\mathrm{d}(\cos\theta)\,\mathrm{d}k \qquad (14.33)$$

and therefore (inserting all pre-factors):

$$\xi(r) = \frac{V}{2\pi^2}\int_0^\infty P(k)\frac{\sin kr}{kr}\,k^2\,\mathrm{d}r \quad \text{(this last Eq. is exact).} \qquad (14.34)$$

For $kr < \pi$: $\sin kr/kr > 0$, while oscillation for $kr > \pi$

$\Longrightarrow$ only wavenumbers $k \lesssim r^{-1}$ contribute to amplitude on scale r.

Power Spectrum: Interpretation

For a power law spectrum,

$$P(k) \propto k^n \qquad (14.35)$$

the correlation function is

$$\xi(r) \propto \int_0^\infty \frac{\sin kr}{kr}k^{n+2}\,\mathrm{d}k \sim \int_0^{1/r} k^{n+2}\,\mathrm{d}k \propto r^{-(n+3)} \qquad (14.36)$$

But the mass within a fluctuation is $M \sim \rho r^3$, i.e., the mass fluctuation spectrum is

$$\xi(M) \propto M^{-(n+3)/3} \qquad (14.37)$$

and therefore the rms density fluctuation at mass scale M is

$$\frac{\delta\rho}{\rho} = \xi(M)^{1/2} \propto M^{-(n+3)/6} \qquad (14.38)$$

For $n > -3$, the rms mass fluctuations decrease with $M \Longrightarrow$ isotropic universe on largest scales

Power Spectrum: Interpretation

What spectra do we expect?

Two simple cases:

Poisson noise: Random statistical fluctuations in number of particles on scale r ("white noise"):

$$\frac{\delta N}{N} = \frac{1}{\sqrt{N}} \quad \Longrightarrow \quad \frac{\delta M}{M} = \frac{1}{\sqrt{M}} \qquad (14.39)$$

and therefore $n = 0$ ($\rho \propto M$!).

Zeldovich spectrum: defined by $n = 1$. Thus

$$\frac{\delta\rho}{\rho} \propto M^{-2/3} \qquad (14.40)$$

...will be important later

The Zeldovich spectrum is the spectrum expected for the case when initial density fluctuations coming through the horizon had the same amplitude.

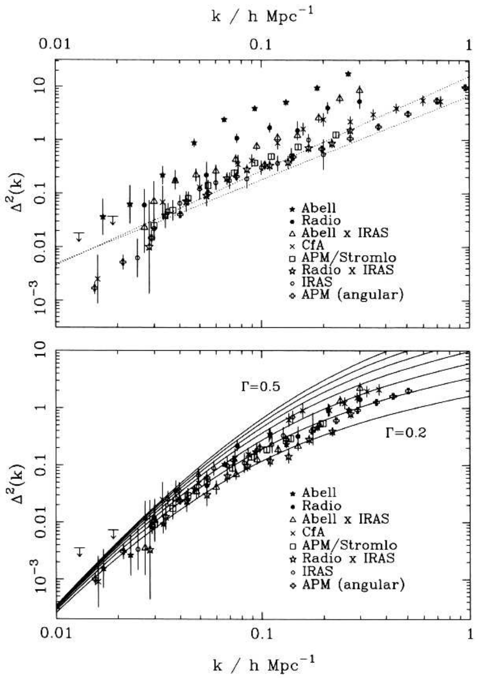

The measured power spectrum is more complicated

$\Longrightarrow$ Structure formation to understand details!

(Peacock, 1999, Fig. 16.4, note that what is shown is $k^3P(k)$ in our notation)

Linear Theory

Structure formation = evolution of overdensity in universe with time.

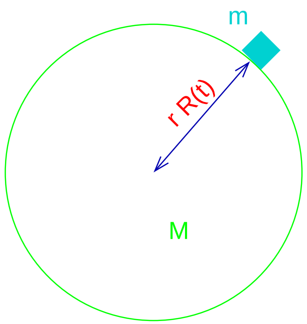

Describe density and scale factor with respect to normal expansion:

$$\rho(t) = \bar{\rho}(t)\cdot(1+\delta(t)) \quad (14.41)$$

$$a(t) = \bar{a}(t)\cdot(1-\epsilon(t)) \quad (14.42)$$

Sign:
$\delta > 0 \Longrightarrow$ *Overdensity*
$\epsilon > 0 \Longrightarrow$ *collapse*
Seek mathematical model for collapse of gravitating material in expanding universe

Question is similar to that used when deriving Friedmann equations.

$\Longrightarrow$ Equation describing structure formation:

$$\dot{a}^2(t) = \frac{8\pi G}{3}\rho(t)a^2(t) + H_0^2(1-\Omega_0) \quad (14.43)$$

We will drop the explicit t dependency in the following

Linear Theory

Onset of structure formation: $\delta(t)$, $\epsilon(t)$ $\ll$ 1 (“linear regime”) $\Longrightarrow$ Ignore all higher orders of δ and ϵ.

Left hand side of Friedmann:

$$\dot{a}^2 = (\dot{\bar{a}} - \dot{\bar{a}}\epsilon - \bar{a}\dot{\epsilon})^2 = \dot{\bar{a}}^2 - 2\dot{\bar{a}}^2\epsilon - 2\bar{a}\dot{\bar{a}}\,\dot{\epsilon} = \dot{\bar{a}}^2 - 2\dot{\bar{a}}\frac{\mathrm{d}}{\mathrm{d}t}(\bar{a}\epsilon) \quad (14.44)$$

Right hand side of Friedmann:

$$\frac{8\pi G}{3}\bar{\rho}(1+\delta)\bar{a}^2(1-\epsilon)^2 + H_0^2(1-\Omega_0) = \frac{8\pi G}{3}\bar{\rho}\bar{a}^2(1+\delta)(1-2\epsilon) + H_0^2(1-\Omega_0)$$
$$= \frac{8\pi G}{3}\bar{\rho}\bar{a}^2(1+\delta-2\epsilon) + H_0^2(1-\Omega_0) \quad (14.45)$$

Therefore Eq. (14.44)=Eq. (14.45):

$$\dot{\bar{a}}^2 - 2\dot{\bar{a}}\frac{\mathrm{d}}{\mathrm{d}t}(\bar{a}\epsilon) = \frac{8\pi G}{3}\bar{\rho}\bar{a}^2(1+\delta-2\epsilon) + H_0^2(1-\Omega_0) \quad (14.46)$$

Use the Friedmann Equation for $\bar{a}$ (Eq. 14.43) to simplify this to

$$-2\dot{\bar{a}}\cdot\frac{\mathrm{d}}{\mathrm{d}t}(\bar{a}\epsilon) = \frac{8\pi G}{3}\bar{\rho}\bar{a}^2(\delta-2\epsilon) \quad (14.47)$$

Linear Theory

To solve Eq. (14.47): Assume for simplicity $\Omega = 1$, matter-dominated universe.

Matter domination $\Longrightarrow \rho a^3 =$ const. $\Longrightarrow$

$$\bar{\rho}(1+\delta)\bar{a}^3(1-\epsilon)^3 \sim \bar{\rho}\bar{a}^3(1-3\epsilon+\delta) \stackrel{!}{=} \text{const.} \quad (14.48)$$

and therefore

$$\epsilon = \delta/3 \quad (14.49)$$

$\Longrightarrow$ Eq. (14.47) becomes

$$-2\dot{\bar{a}}\cdot\frac{\mathrm{d}}{\mathrm{d}t}(\bar{a}\delta) = \frac{8\pi G}{3}\bar{\rho}\bar{a}^2\delta \quad (14.50)$$

In a $k=0$ universe,

$$\bar{a}(t) = \left(\frac{3H_0}{2}t\right)^{2/3} =: a_0t^{2/3} \quad (7.72)$$

and because of $\rho a^3 =$ const.,

$$\bar{\rho}(t) \propto t^{-2} =: \rho_0 t^{-2} \quad (14.51)$$

Linear Theory

Insert $\bar{a}$, $\bar{\rho}$ into Eq. (14.50):

$$-\frac{4a_0}{3}t^{-1/3}\left(\frac{2a_0}{3}t^{-1/3}\delta + a_0t^{2/3}\dot{\delta}\right) = \frac{8\pi G}{3}\rho_0 t^{-2}a_0^2 t^{4/3}\delta \qquad (14.52)$$

and simplify

$$-t^{-2/3}\delta - t^{1/3}\dot{\delta} = 2\pi G\rho_0 t^{-2/3}\delta \qquad (14.53)$$

which gives

$$t\dot{\delta} + (1 + 2\pi G\rho_0)\delta = 0 \qquad (14.54)$$

The general solution of Eq. (14.54) is a power-law

$\Longrightarrow$ Growth of structure!

Since also *negative* PL indexes possible

$\Longrightarrow$ Some initial perturbations can be damped out!

We need a better theory to do that in detail. . .

A better derivation of the Jeans length comes from considering the evolution of a fluid in an expanding universe. Assuming that the initial density perturbations were small, we can use perturbation theory for obtaining deviations from homogeneity (=structures).

In a Friedmann universe, for length scales $< 1/H$, dynamical equations are Newtonian to first order, but we need to still use the scale factor, $a(t)$ in the fluid equations.

Continuity equation:

$$\dot{\rho} + \nabla\cdot(\rho\mathbf{v}) = 0 \qquad (14.58)$$

Euler's equation:

$$\dot{\mathbf{v}} + (v\cdot\nabla)v = -\nabla\left(\Phi + \frac{\rho}{c}\right) \qquad (14.59)$$

Poisson's equation:

$$\nabla^2\Phi = 4\pi G\rho \qquad (14.60)$$

Without perturbations (i.e., the zeroth order solution) is given by the normal Friedmann solutions:

$$\rho_0(t,\mathbf{r}) = \frac{\rho_0}{a^3(t)} \quad \text{(dilution by expansion)} \qquad (14.61)$$

$$\mathbf{v}_0(t,\mathbf{r}) = \frac{\dot{a}(t)}{a(t)}\mathbf{r} \quad \text{(Hubble law)} \qquad (14.62)$$

$$\Phi_0(t,\mathbf{r}) = \frac{2\pi G\rho_0 r^2}{3} \quad \text{(soln. of Poisson with } \rho = \text{const.)} \qquad (14.63)$$

Convert into comoving coordinates ($\mathbf{x} = \mathbf{r}/a(t)$) to get rid of the $a(t)$'s and write down perturbation equations:

$$\rho(t,\mathbf{x}) = \rho_0(t) + \rho_1(t) =: \rho_0(t)\,(1 + \delta(t,\mathbf{x})) \qquad (14.64)$$

$$\mathbf{v}(t,\mathbf{x}) = \mathbf{v}_0(t,\mathbf{x}) + \mathbf{v}_1(t,\mathbf{x}) \qquad (14.65)$$

$$\Phi(t,\mathbf{x}) = \Phi_0(t,\mathbf{x}) + \Phi_1(t,\mathbf{x}) \qquad (14.66)$$

where $|\delta|$, $|\mathbf{v}_1|$, $|\Phi_1|$ small (δ is called density perturbation field).

Since the equations are spatially homogeneous, we can Fourier transform them to search for plane wave solutions. The general perturbation solution can then later be found by performing linear combinations of these plane waves.

$$\delta(t,\mathbf{x}) = \frac{1}{(2\pi)^3}\int e^{i\mathbf{k}\cdot\mathbf{x}}\delta(t,\mathbf{k})d^3k \Longleftrightarrow \delta(t,\mathbf{k}) = \int e^{-i\mathbf{k}\cdot\mathbf{x}}\delta(t,\mathbf{x})d^3x \qquad (14.67)$$

Inserting into hydro equations gives

$$\ddot{\delta}(t,\mathbf{k}) + 2\frac{\dot{a}(t)}{a(t)}\dot{\delta}(t,\mathbf{k}) + \left(\frac{k^2c_s^2}{a^2(t)} - 4\pi G\rho_0\right)\delta(t,\mathbf{k}) = 0 \qquad (14.68)$$

Linear Theory

Better linear theory: Use linearized equations of motion from hydrodynamics.

Detailed theory very difficult, see handout for a few ideas of what is going on. . .

Classical approach, considering a collapsing sphere:

Potential energy and kinetic energy content of sphere:

$$U = -\frac{1}{2}\int \rho(x)\Phi(x)\,d^3x \sim -\frac{16\pi^2}{15}G\rho^2 r^5 \quad \text{and} \quad T \sim \frac{c_s^2}{2}\frac{4\pi r^3\rho}{3} \qquad (14.55)$$

c_s: speed of sound; for neutral Hydrogen, $c_s = \sqrt{5T/3m_p}$.

Sphere collapses for $|U| > T$, i.e., when

$$2r \gtrsim \sqrt{\frac{5}{2\pi}}\sqrt{\frac{c_s^2}{G\rho}} \sim c_s\sqrt{\frac{\pi}{G\rho}} =: \lambda_J \qquad (14.56)$$

λ_J is called the Jeans length, the corresponding mass is the Jeans mass,

$$M_J = \frac{\pi}{6}\rho\lambda_J^3 \qquad (14.57)$$

Structures with $m < M_J$ cannot grow.

Note that c_s is time dependent $\Longrightarrow M_J$ can change with time!

where the sound speed is $c_s^2 = (\partial p/\partial\rho)_{\text{adiabatic}}$.

Solutions to Eq. 14.68 grow or decrease depending on sign of

$$\kappa_J = \left(\frac{k^2c_s^2}{a^2(t)} - 4\pi G\rho_0\right) \qquad (14.69)$$

Thus, growth is only possible for $k > k_J$ where

$$k_J = \sqrt{\frac{4\pi G\rho_0 a^2(t)}{c_s^2}} \qquad (14.70)$$

or, in terms of physical wavelengths,

$$\lambda_J = \frac{2\pi a(t)}{k_J} = c_s\sqrt{\frac{\pi}{G\rho_0}} \qquad (14.71)$$

the Jeans length.

Classical Structure Formation

Early universe: radiation dominates:

$$c_s = c/\sqrt{3} \quad \text{and} \quad \rho_r c^2 = \sigma T^4 \tag{14.72}$$

and therefore

$$\lambda_{J,rad} = c^2\sqrt{\pi/3G\sigma T^4} \propto \rho_r^{-1/2} \propto a^2 \quad \text{and} \quad M_J \propto \rho_m \lambda_{J,rad}^3 \propto a^3 \tag{14.73}$$

In the early universe, the Jeans mass grows quickly.

At time of radiation – matter equilibrium,

$$\rho_m = \rho_{rad} = \sigma T_{eq}^4/c^2 \tag{14.74}$$

and

$$M_J(t_{eq}) = \frac{\pi^{5/2}}{18\sqrt{3}}\frac{c^4}{G^{3/2}\sigma^{1/2}}\frac{1}{T_{eq}} \sim \frac{3.6\times10^{16}(\Omega_0 h^2)^{-2}\,M_\odot}{(T/T_{eq})^3} \tag{14.75}$$

assuming $1+z_{eq} = 24000\,\Omega_0 h^2$.

$\Longrightarrow$ much larger than mass in galaxy cluster ($\sim$ mass of $(50\,\text{Mpc})^3$-cube)
Overdense regions with $m < M_{J,rad}$ are smoothed out by the radiation coupling to matter.

Much larger structures also cannot grow since λ is larger than horizon radius $\Longrightarrow$ Mass spectrum of possible structures.

Classical Structure Formation

After t_{eq} not much happens until $T_{rec} \sim 3000\,\text{K}$

$\Longrightarrow$ recombination

$\Longrightarrow$ Sound speed drops dramatically (radiation and matter decouple):

$$c_s \sim \frac{kT}{m_p} \sim 5\,\text{km}\,\text{s}^{-1} \tag{14.76}$$

$\Longrightarrow$ M_J drops by 10^{11}:

$$M_{J,eq} = \frac{\pi\bar{\rho}}{6}\left(\frac{\pi k T_{rec}}{G\bar{\rho}m_p}\right)^{1/2} \sim 5\times10^5(\Omega_0 h^2)^{-1/2}\,M_\odot \tag{14.77}$$

after that, M_J drops because of expansion.

So, in a pure matter universe: huge structures (Zeldovich pancakes) form early, and then fragment at recombination. $\Longrightarrow$ "top-down model"

Problem: This is not really what has been observed (i.e., galaxy clusters are not yet fully formed, but galaxies are)

Solution: Dark matter

Structure Formation and DM

Structure formation with dark matter:

DM unaffected by radiation pressure $\Longrightarrow$ collapse of smaller structures possible

$\Longrightarrow$ bottom-up model

As long as DM is relativistic:

$$M_{J,HDM} = \frac{\pi\rho_{DM}}{6}\left(\frac{\pi c_{DM}}{G\rho_{DM}}\right)^{3/2} \tag{14.78}$$

Hot Dark Matter: $c_{HDM} \sim c/\sqrt{3}$

Cold Dark Matter: $c_{CDM} \ll c/\sqrt{3}$

Standard CDM Scenario:

- DM cools long before t_{rec}
- CDM structures form, M_J about galaxy mass, while baryons coupled to radiation $\Longrightarrow$ stays smooth
- t_{rec}: matter decouples, falls in DM gravity wells

CDM "seeds" structures!

Gives not exactly observed power spectrum

$\Longrightarrow$ Currently preferred: combination of CDM and ΛDM

Structure Formation and DM

Finally, the *real* linear theory has to be done in linearized or even full general relativity

$\Longrightarrow$ very, very complicated.

Full fledged, detailed structure formation is mainly done numerically.

N-body codes: describe particles (=galaxies) as points, compute mutual interactions in expanding universe

Requires massive computing power.

VIRGO consortium: USA, Canada, Germany, UK

Hubble Volume Simulation: Garching T3E (512 processors), 70 h CPU time

followed by the Millenium Simulation (30 d CPU time)

see Springel et al. (2005), Springel et al. (2006) and
`http://www.mpa-garching.mpg.de/~virgo/virgo/`

The Hubble Volume Simulation

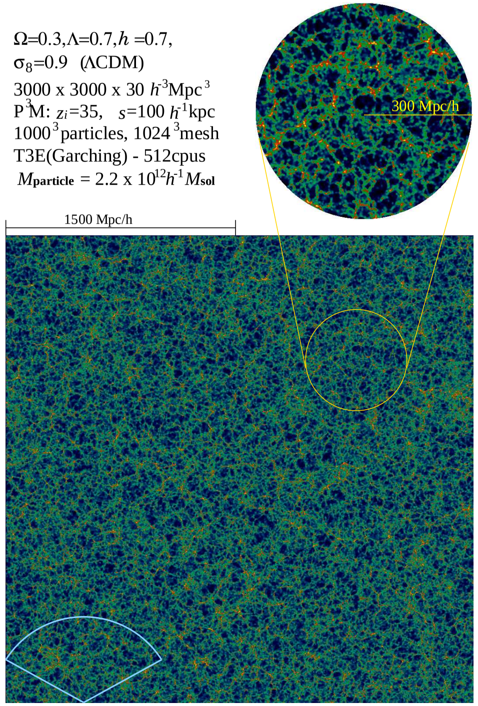

ΛDM, pie shows SDSS size

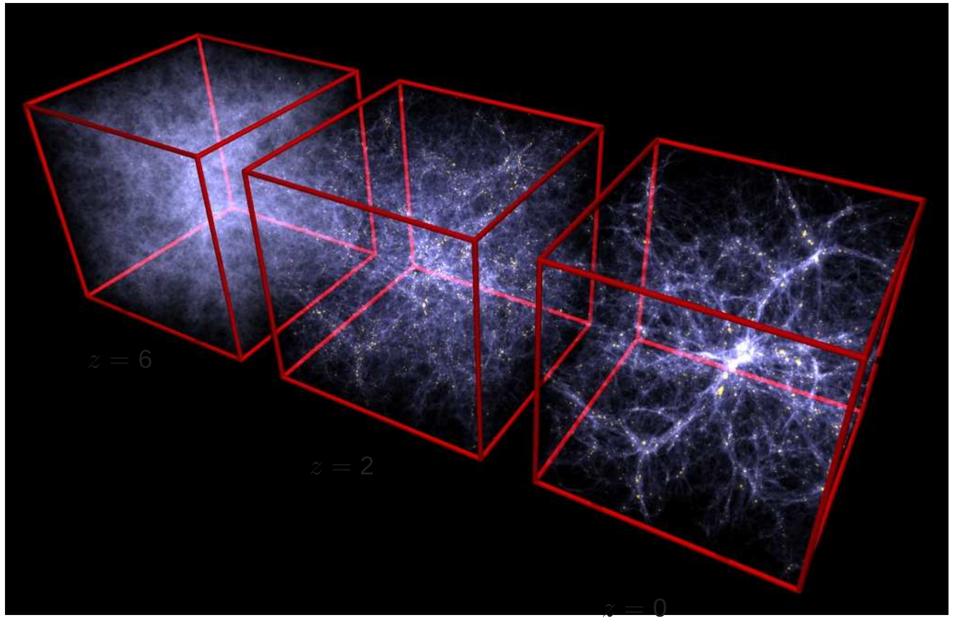

(V. Springel/MPA)

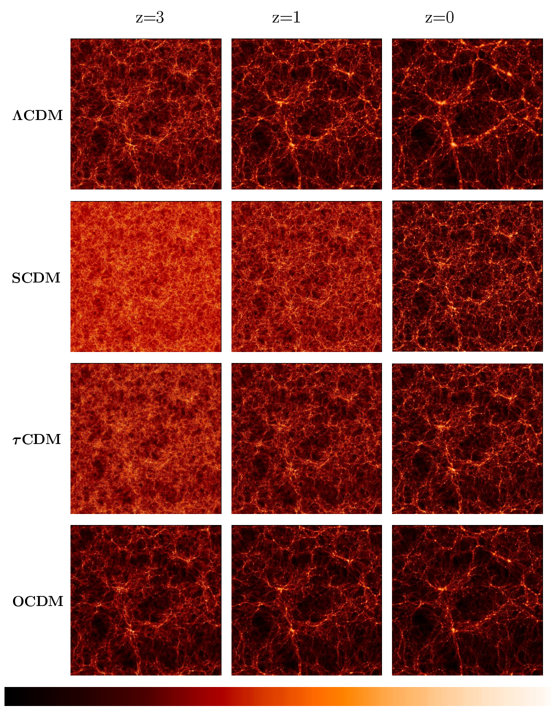

The VIRGO Collaboration 1996

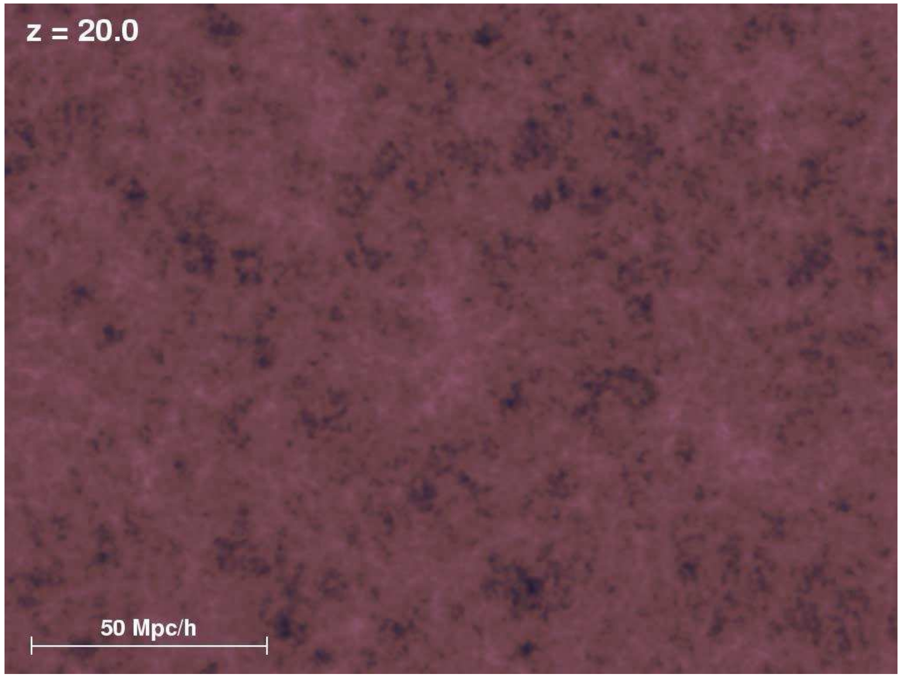

Evolution of structure in a ΛCDM Universe (MPA/V. Springel)

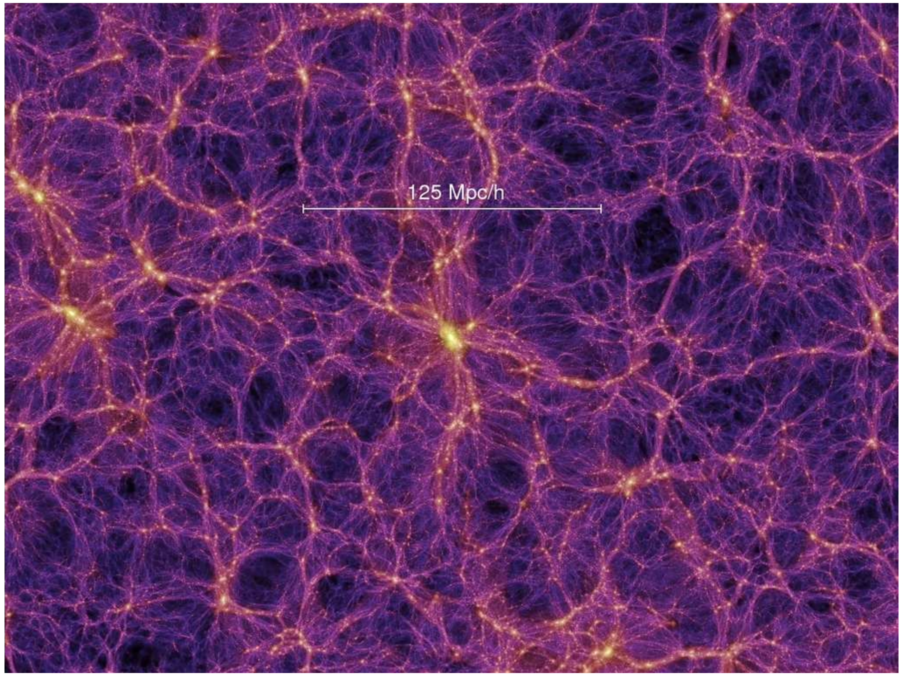

Todays dark matter distribution. . . (V. Springel/MPA)

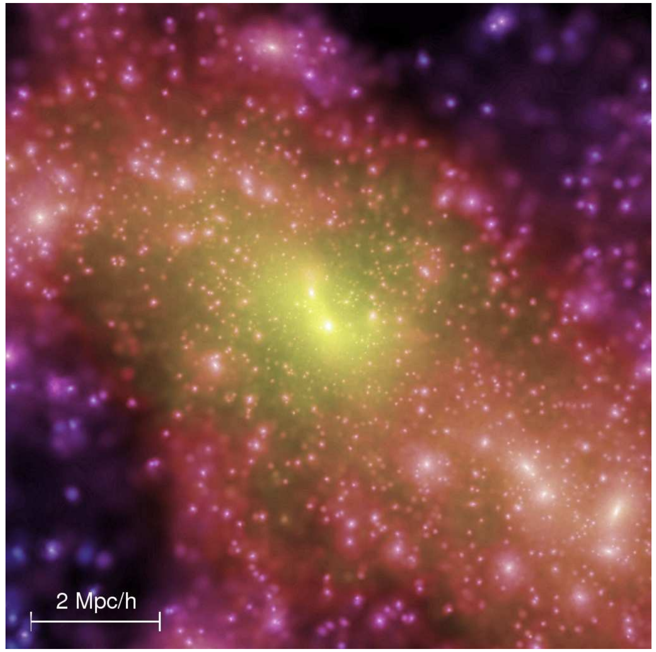

Todays dark matter distribution in a cluster. . . (V. Springel/MPA)

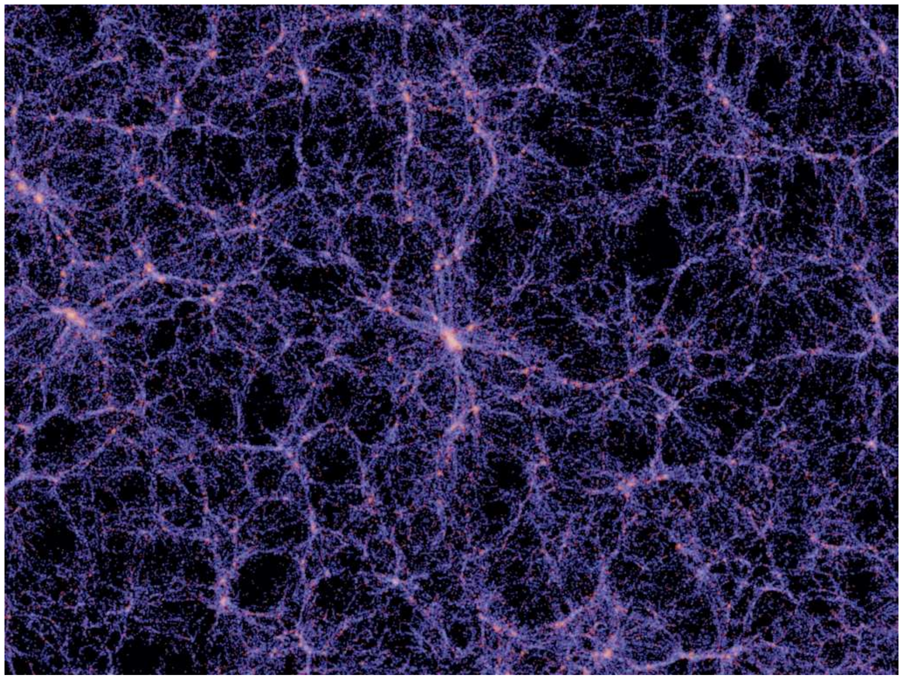

. . . and corresponding galaxy distribution (V. Springel/MPA)

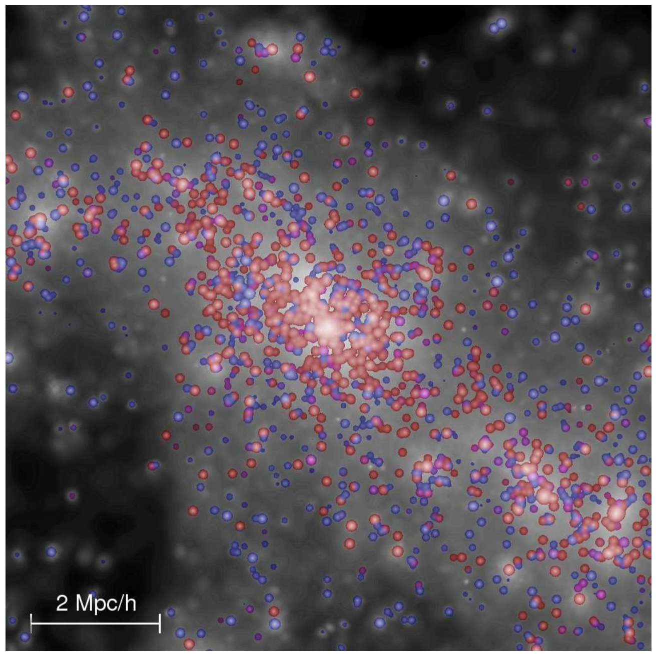

. . . and corresponding galaxy distribution (V. Springel/MPA)

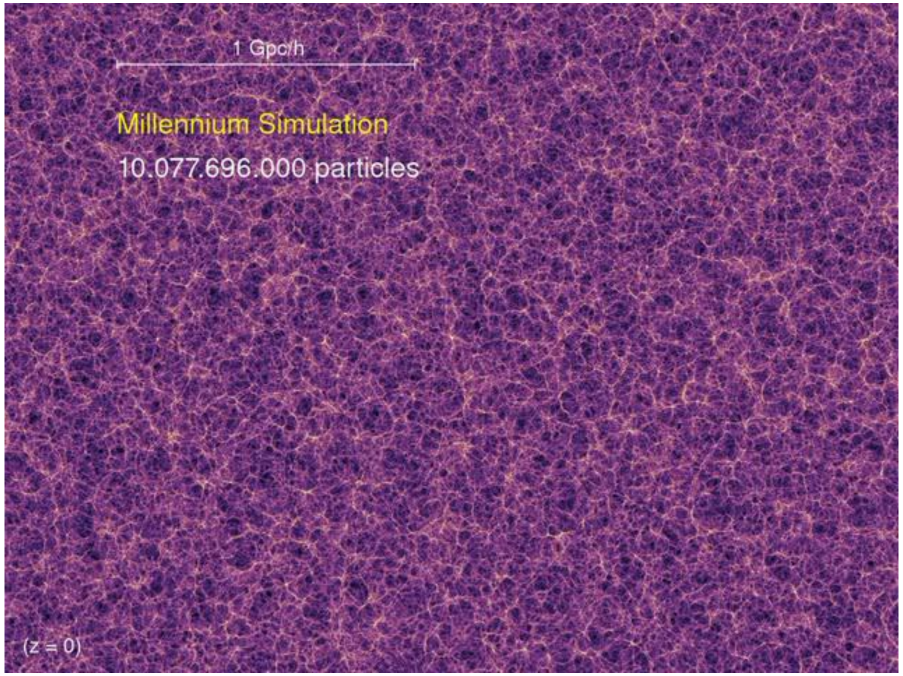

Zoom into the DM structure of the Millennium Simulation

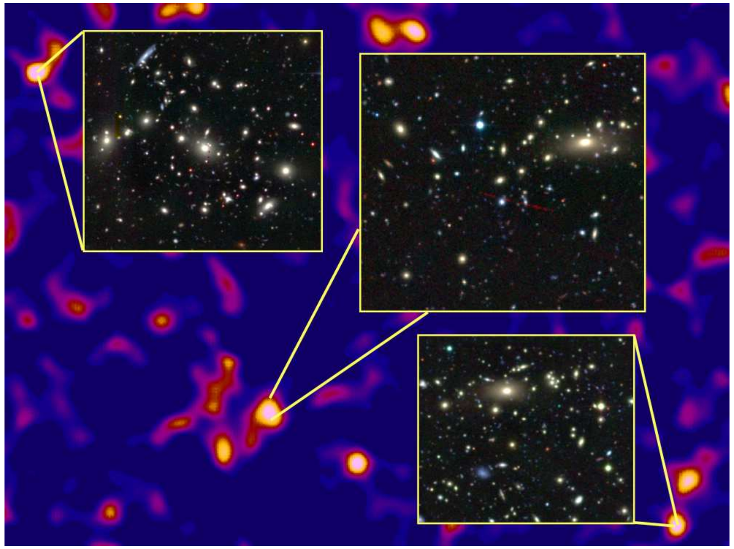

Van Waerbeke, Heymans, and CFHTLens collaboration

DM Distribution from CFHTLens project (spring 2011 region)

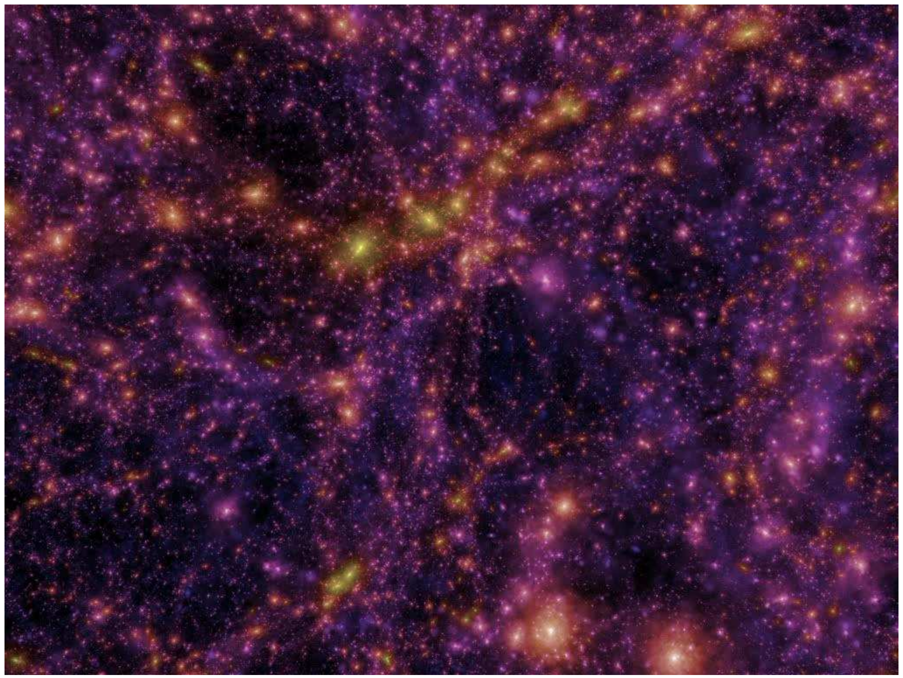

Flight through the DM structure of the Millennium Simulation (V. Springel)

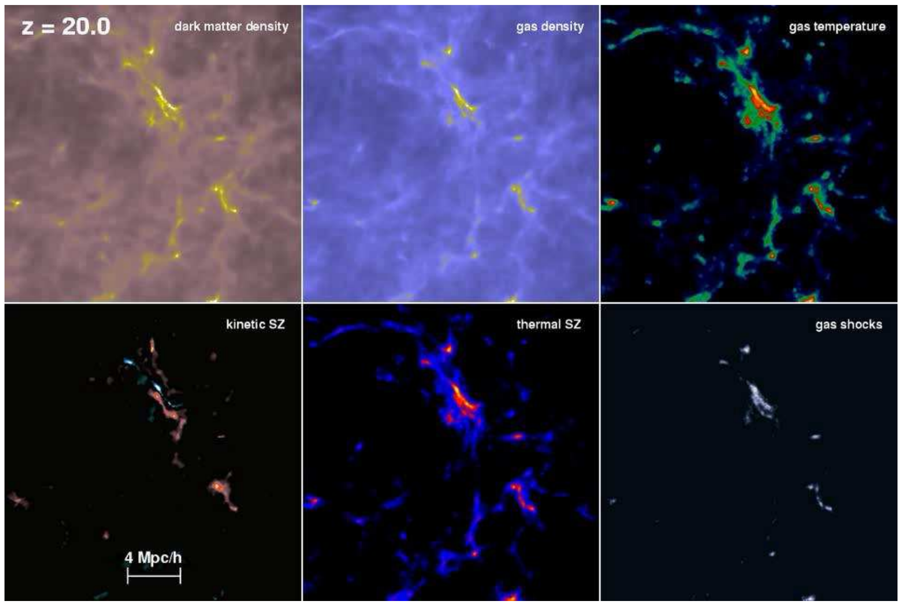

Formation of a galaxy cluster (V. Springel)

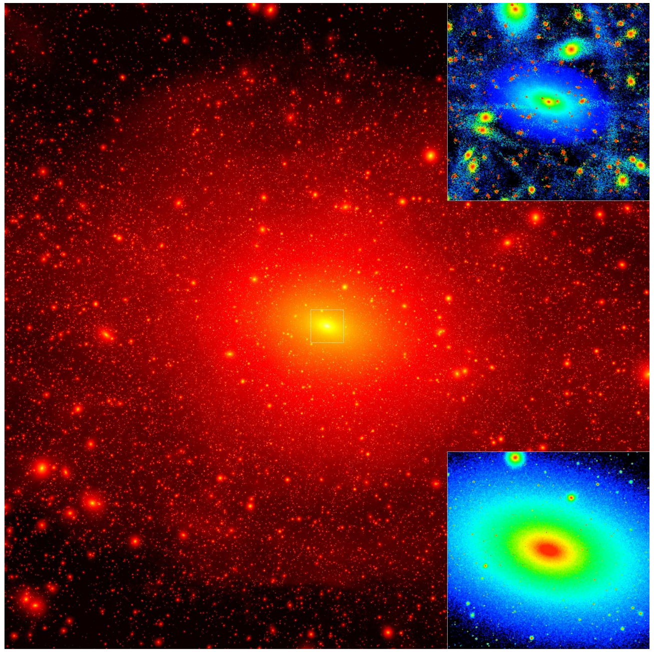

Via Lactea project: Dark Matter Halo around a galaxy
movies: `vl_form_inset.mpg`

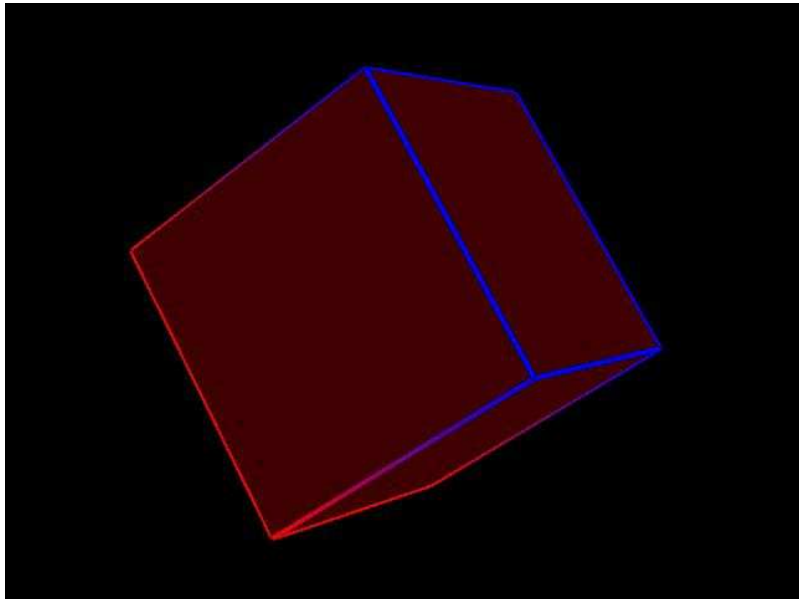

(movie courtesy N. Gedin)

Reionization

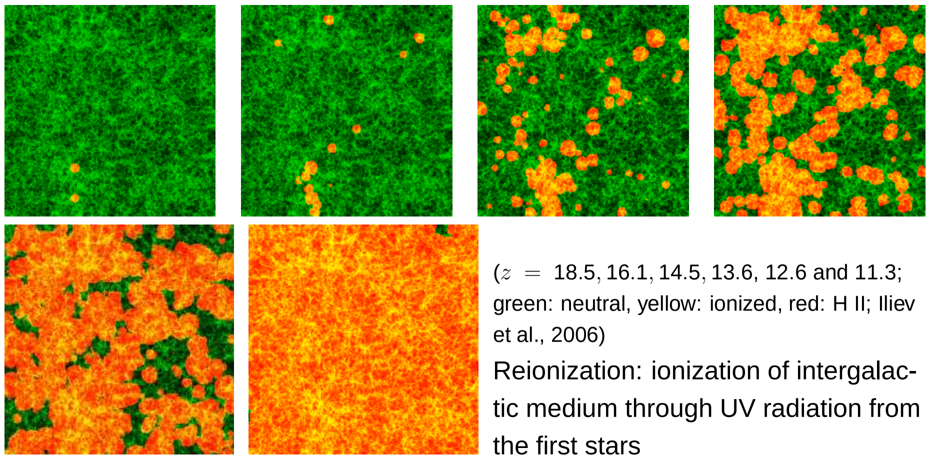

(z = 18.5, 16.1, 14.5, 13.6, 12.6 and 11.3; green: neutral, yellow: ionized, red: H II; Iliev et al., 2006)

Reionization: ionization of intergalactic medium through UV radiation from the first stars

movie: `xy_f2000_250s_406_wmap3.gif`

Formal Structure Formation

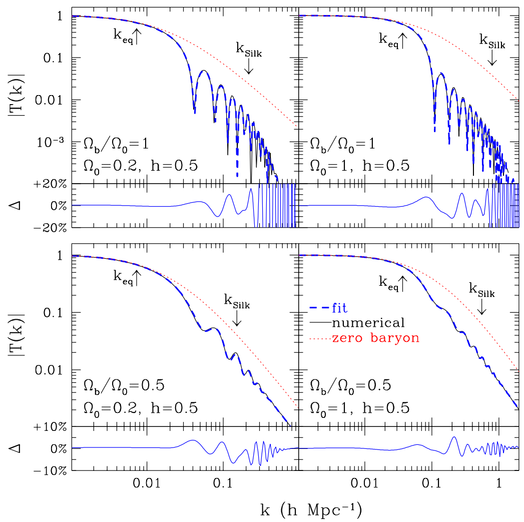

Calculation of real power spectra difficult: growth under self-gravitation pressure effects dissipation.

To predict observations from today: define transfer function

$$\delta_k(z=0) = D(z)T_k\delta_k(z) \quad (14.79)$$

But: need initial conditions, $\delta_k(z)$!

(Eisenstein & Hu, 1999)

CMBR

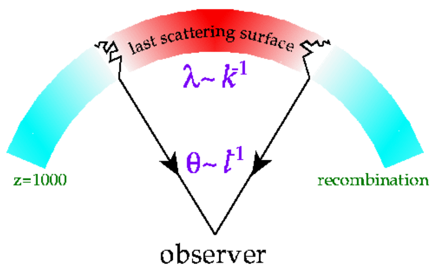

courtesy Wayne Hu

Matter and Radiation are coupled, i.e., large mass density = high photon density.

Photons from overdense regions: gravitational redshift $\Longrightarrow$ observable! (Sachs Wolfe Effect)

CMBR: Radiation from surface of last scattering $\Longrightarrow$ Gravitational redshift is observable as temperature fluctuation:

$$\frac{\Delta T}{T} \sim \frac{\Delta\Phi_\mathrm{g}}{c^2} \qquad (14.80)$$

CMBR Fluctuations trace gravitational potential at $z \sim 1100$!

CMBR

Temperature fluctuations:

$$\frac{\Delta T}{T} \sim \frac{\Delta\Phi_\mathrm{g}}{c^2} \qquad (14.80)$$

where

$$\Delta\Phi_\mathrm{g} \sim -\frac{2G\Delta M}{R} = \frac{8\pi G}{3}\bar{\rho}R^2\delta = -\delta(t)\,(H(t)R)^2 \qquad (14.81)$$

Current angle of region on sky:

$$\alpha \sim R/d_\mathrm{A} \qquad (14.82)$$

where the angular diameter distance

$$d_\mathrm{A} = d_\mathrm{L}/(1+z)^2 \qquad (14.83)$$

Therefore:

$$\frac{\Delta T}{T} \sim \frac{\Delta\Phi_\mathrm{g}}{c^2} \propto -\frac{\delta\alpha^2}{3} \qquad (14.84)$$

Quotient 3 from more detailed theory, "Integrated Sachs Wolfe effect"

CMBR

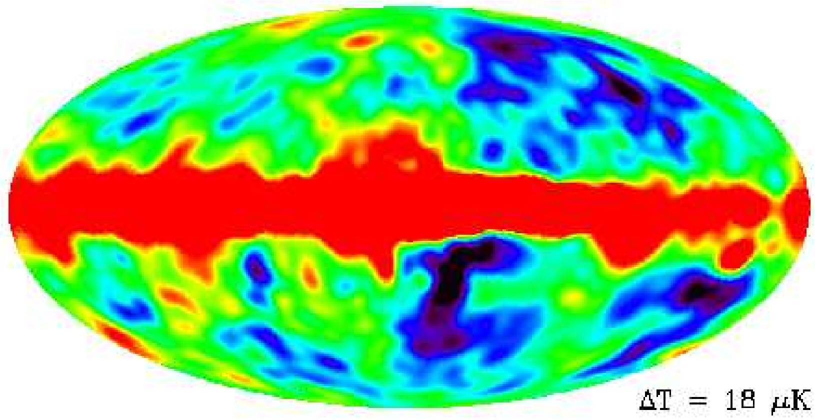

COBE: Resolution $\alpha \sim 7^\circ$ (corresponds to $\sim 10^{20}\,M_\odot$ at recombination). Temperature fluctuations imply $\delta \sim 10^{-3}$ at recombination.

This is small for pure matter dominated universe $\Longrightarrow$ Implies existence of dark matter!

CMBR

Detailed theory of fluctuations: Expand CMB fluctuations on sky in spherical harmonics:

$$\frac{\Delta T}{T}(\theta,\phi) = \sum_{\ell,m} a_{\ell,m}Y_{\ell,m}(\theta,\phi) \qquad (14.85)$$

Since rotationally symmetric, can express variation in terms of multipole coefficients, C_ℓ:

$$C(\theta) = \frac{1}{4\pi}\sum_{\ell}\sum_{m=-\ell}^{+\ell}|a_{\ell,m}|P_\ell(\cos\theta) \qquad (14.86)$$

$$=: \frac{1}{4\pi}\sum_{\ell}(2\ell+1)C_\ell P_\ell(\cos\theta) \qquad (14.87)$$

where $C(\theta) = \langle\Delta T/T\rangle$ and where the P_ℓ are the Legendre polynomials.

CMBR

Expect following features:

Large angle anisotropy: (small ℓ, scales $\gtrsim$ horizon at decoupling): Flat part due to Sachs-Wolfe effect

Smaller angular scales: (larger ℓ): Influenced by photon-baryon interactions:

Matter falls in potential well

$\Longrightarrow$ Pressure resists

$\Longrightarrow$ acoustic oscillations

$\Longrightarrow$ Power at selected scales!

Power from those density fluctuations which had their maximum amplitude at time of last scattering dominates $\Longrightarrow$ acoustic peak

Also damping from photon diffusion (Compton scattering; Silk damping [after Joseph Silk])

courtesy BOOMERANG team

Enter: BOOMERANG (Balloon Observations of Milimetric Extragalactic Radiation and Geophysics), Flight in Antarctica 1998 December 29 – 1999 January 9

CMBR

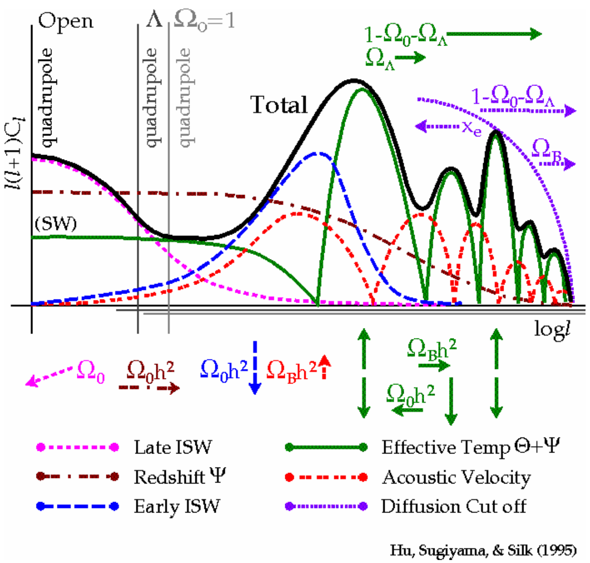

Location and strength of acoustic peaks dependent on

$$\Omega_b \quad H_0 \quad \Omega_0$$

Position of acoustic peak not observed with COBE (at smaller scale than 7°)

BOOMERANG before Mt. Erebus; courtesy BOOMERANG team

Other balloon missions: MAXIMA-1,. . .

Summary: Pre-WMAP

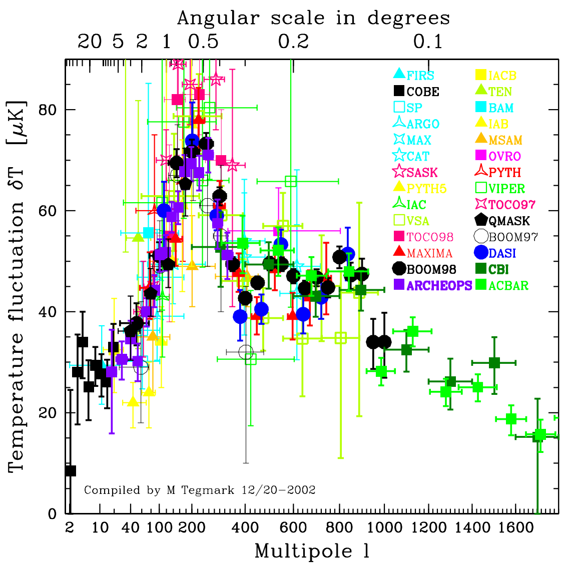

1st acoustic peak found by BOOMERANG in 1999

(Jaffe et al., 2000)

Courtesy M. Tegmark

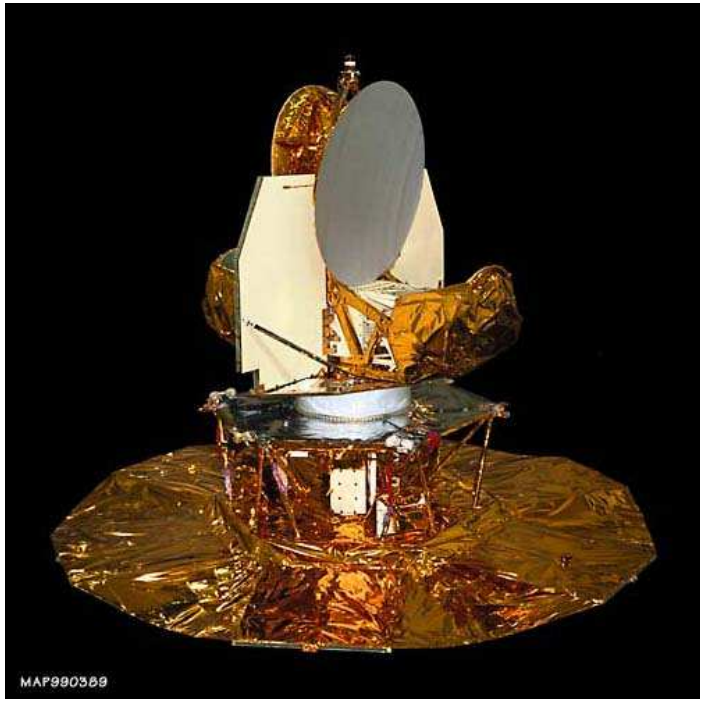

Wilkinson Microwave Anisotropy Probe (WMAP):

- Launched 2001 June 30, measurements began 2001 August 10
- Orbit around 2nd Lagrange Point of Sun-Earth System
- Highly precise radiometers of high spatial resolution (best: 0.21° FWHM in W-Band at 3.2 mm) in five wavebands

(see Bennett et al. 2003 for an overview).

Summary: Pre-WMAP

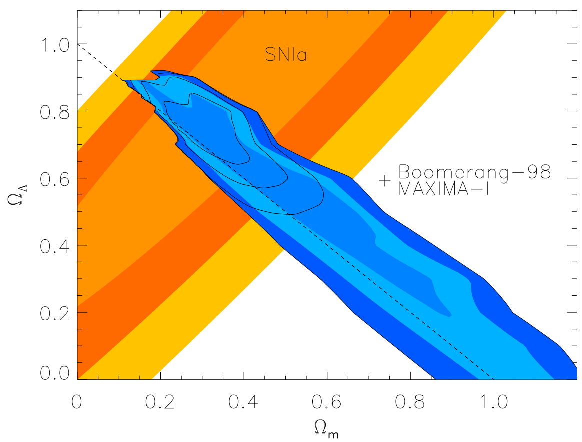

(Jaffe et al., 2000, black contours: incl. Large Scale Structure)

Summary of CMB fluctuations pre 2000 (COBE, BOOMERANG, MAXIMA):

$$\Omega_{tot} \simeq 1.11 \pm 0.07 \left({}^{+0.13}_{-0.12}\right) \quad \Omega_b h^2 \simeq 0.032^{+0.005}_{-0.004} \left({}^{+0.009}_{-0.008}\right) \tag{14.88}$$

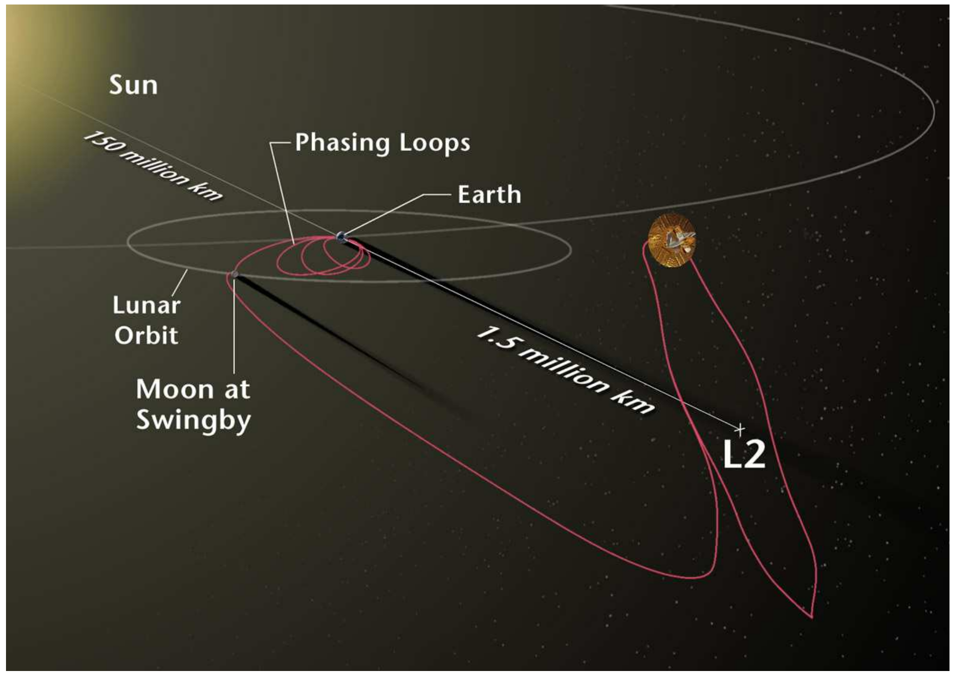

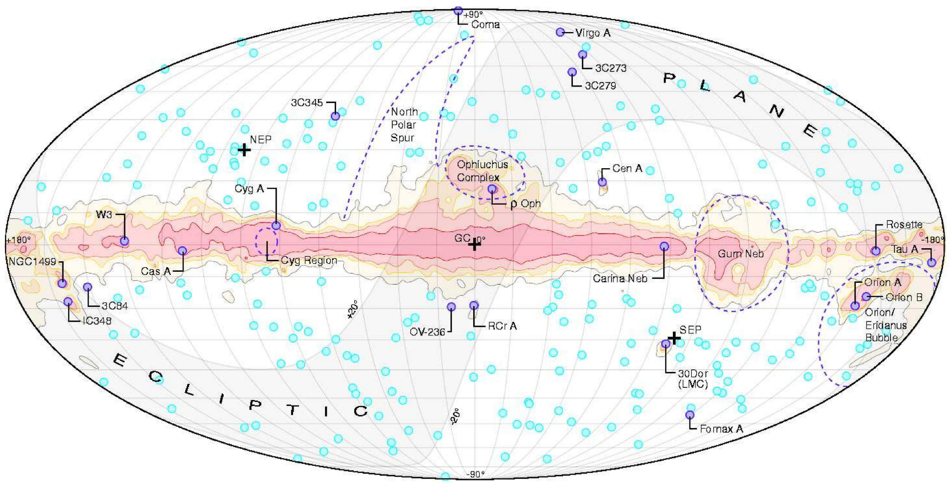

Foreground features of the microwave sky (Bennett et al., 2003).

Sunyaev Zeldovich effect is expected to be strongest in Coma cluster, temperatures of -0.34 ± 0.18 mK in W and -0.24 ± 0.18 mK in K-band; barely detectable with WMAP, does not contaminate maps.

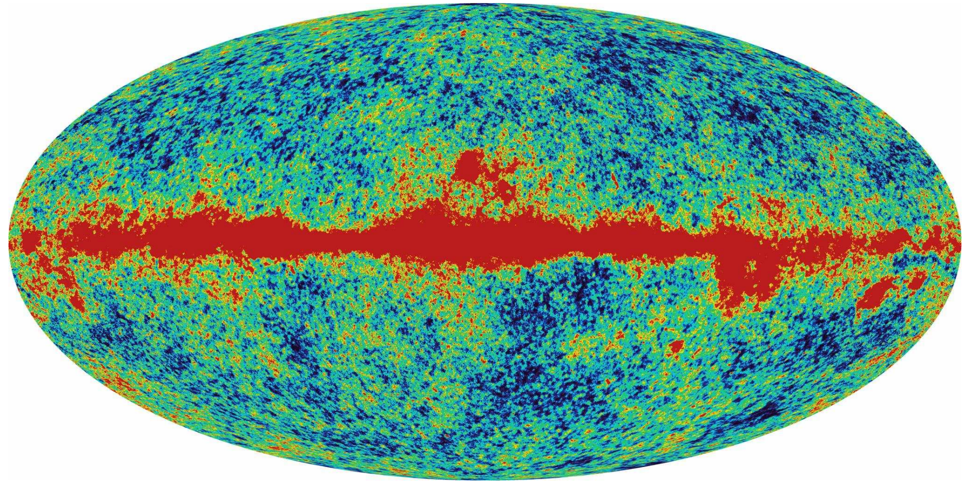

WMAP, Q-Band, $\lambda = 7.3$ mm, $\nu = 40.7$ GHz, $\theta = 0.49^\circ$ FWHM

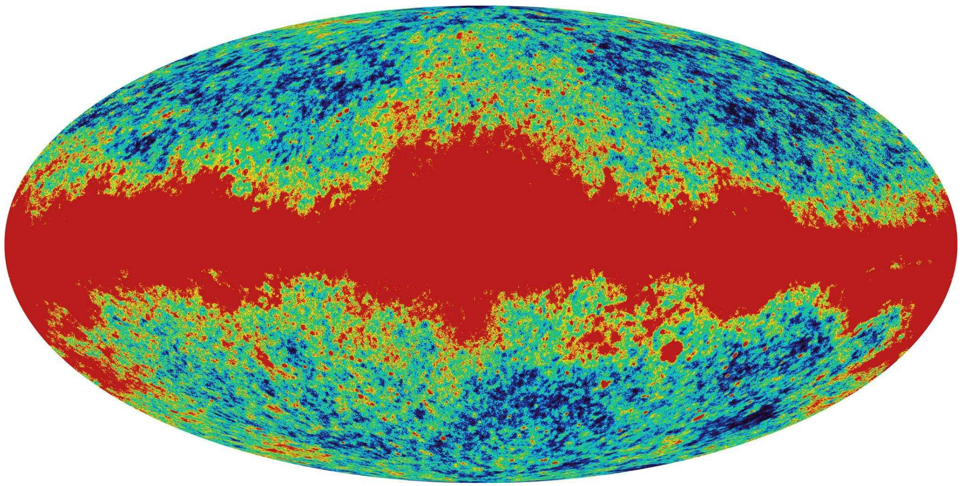

WMAP, K-Band, $\lambda = 13$ mm, $\nu = 22.8$ GHz, $\theta = 0.83^\circ$ FWHM

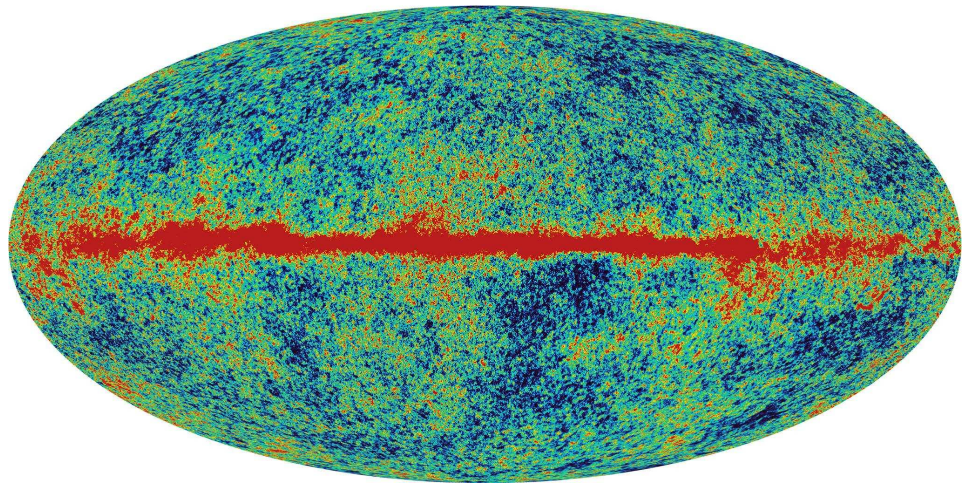

WMAP, W-Band, $\lambda = 3.2$ mm, $\nu = 93.5$ GHz, $\theta = 0.21^\circ$ FWHM

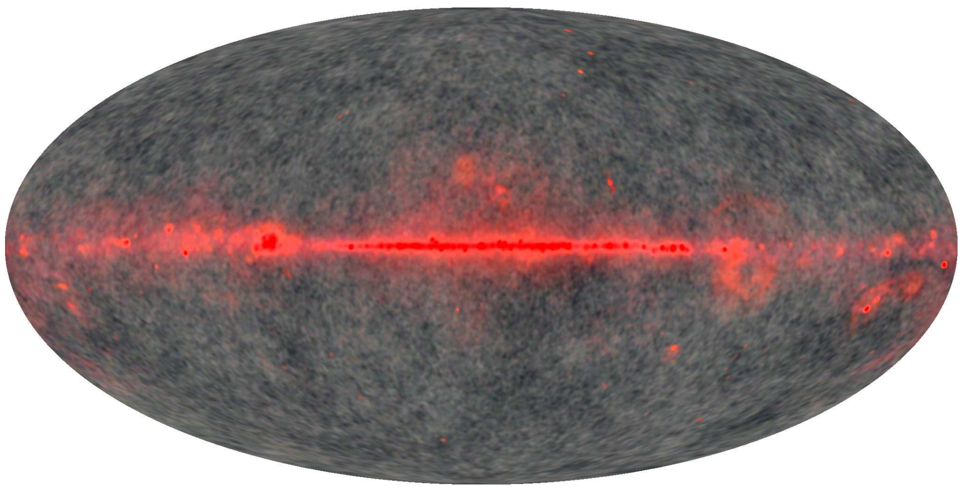

Different spectral signature enables identification of Galaxy foreground radiation

Power Spectrum

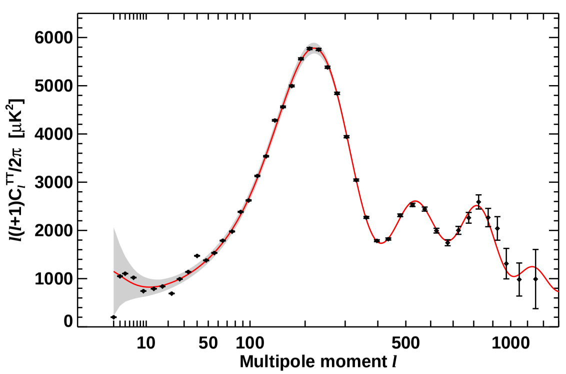

(WMAP, 7 year data; Larson et al., 2010, Fig. 1)

Best fit parameters for WMAP data after 7 years of measurements (Jarosik et al., 2010):

$$h = 0.704(14)$$
$$\Omega_b = 0.0456(16)$$
$$\Omega_c = 0.227(14)$$
$$\Omega_\Lambda = 0.728(16)$$
$$\Omega_{tot} = 1.0023^{+0.0056}_{-0.0054}$$
$$\tau_{reion} = 0.089 \pm 0.030$$
$$\text{Age} = 13.75(11)\,\text{Gyr}$$

Ω_c: Ω in dark matter.

Power spectrum requires that Λ behaves like a cosmological constant.

$\Longrightarrow$ Very good agreement between data and theory!

Outlook: *Planck*

May 14, 2009: Launch of the *Planck* satellite (together with *Herschel*).

- Mapping the CMB with micro-Kelvin sensitivity ($\Delta T/T = 10^{-6}$).
- Better separation of CMB from Galactic and extragalactic foreground radiation through multi-frequency mapping (27 GHz – 1 THz).
- Detect CMB anisotropies in polarized emission.
- First science results published in January 2011.
- Detector ran out of coolant in January 2012

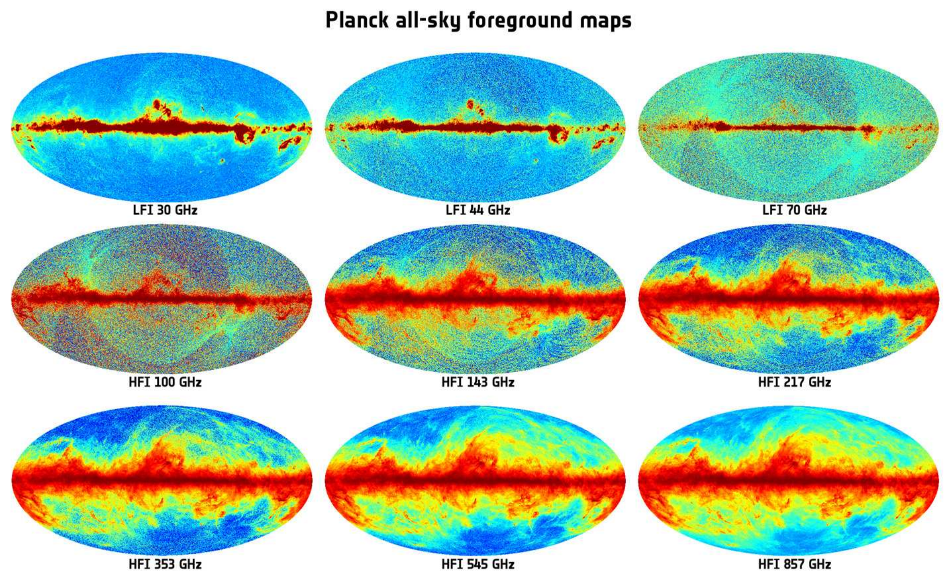

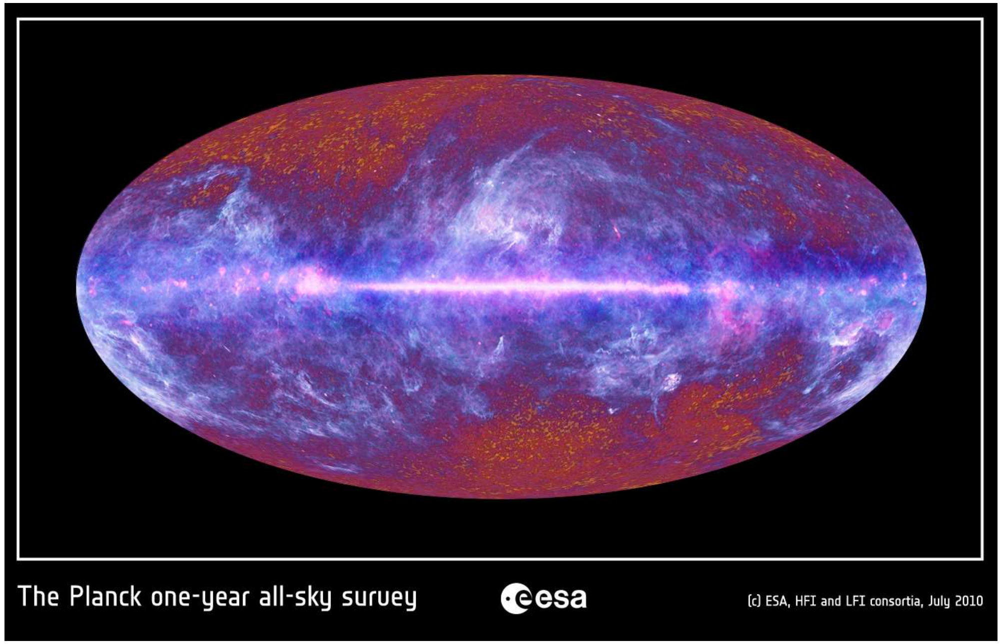

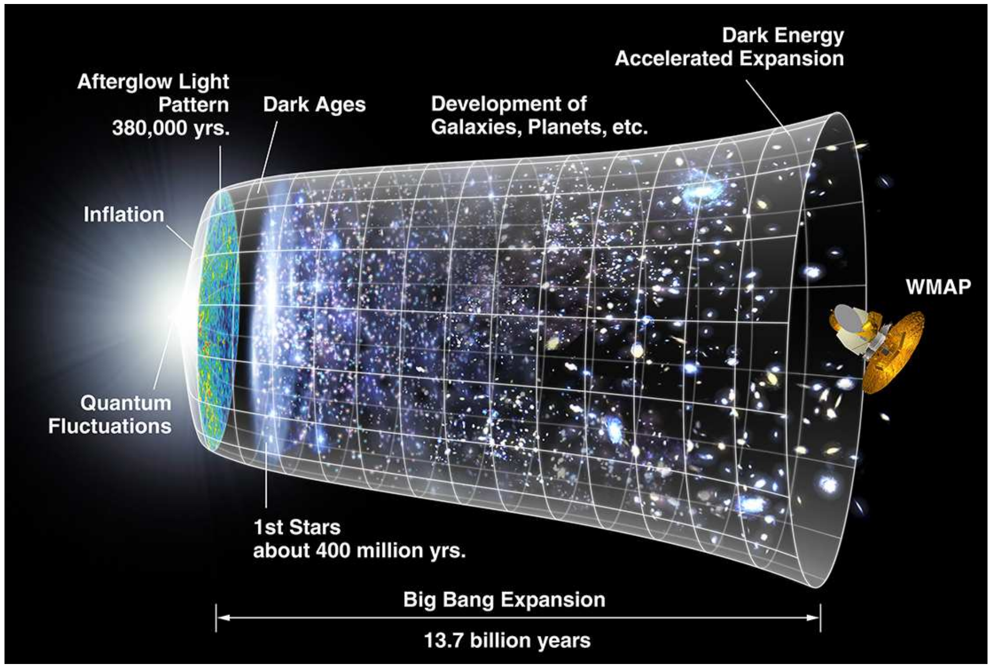

Credit: NASA/WMAP Science Team

Bahcall, N. A., & Soneira, R. M. 1983, ApJ, 270, 20

Bennett, C. L., Halpern, M., Hinshaw, G., et al. 2003, ApJ, submitted

Cole, S., Percival, W. J., Peacock, J. A., et al. 2005, MNRAS, 362, 505

de Lapparent, V., Geller, M. J., & Huchra, J. P. 1986, ApJ, 302, L1

Eisenstein, D. J., & Hu, W. 1999, ApJ, 511, 5

Hamilton, A. J. S., & Tegmark, M. 2002, MNRAS, 330, 506

Iliev, I. T., Mellema, G., Pen, U.-L., et al. 2006, MNRAS, 369, 1625

Jaffe, A. H., Ade, P. A. R., Balbi, A., et al. 2000, Phys. Rev. Lett., submitted (astro-ph/0007333)

Jarosik, N., Bennett, C. L., Dunkley, J., et al. 2010, ApJ, in press (arXiv:1001.4744)

Larson, D., Dunkley, J., Hinshaw, G., et al. 2010, ApJ, in press (arXiv:1001.4635)

Peacock, J. A., 1999, Cosmological Physics, (Cambridge: Cambridge Univ. Press)

Peebles, P. J. E., 1980, The Large-Scale Structure of the Universe, (Princeton, NJ: Princeton Univ. Press)

Spergel, D. N., Bean, R., Doré, O., et al. 2007, ApJS, 170, 377

Spergel, D. N., Verde, L., Peiris, H. V., et al. 2003, ApJ, submitted

Springel, V., Frenk, C. S., & White, S. D. M. 2006, Nature, 440, 1137

Springel, V., White, S. D. M., Jenkins, A., et al. 2005, Nature, 435, 629

Strauss, M. A., 1999, in Structure Formation in the Universe, ed. A. Dekel, J. P. Ostriker, (Cambridge: Cambridge Univ. Press)

Strauss, M. A., & Willick, J. A. 1995, Phys. Rep., 261, 271

Tegmark, M., Blanton, M. R., Strauss, M. A., et al. 2004, ApJ, 606, 702

Tucker, D. L., Oemler, A., Kirshner, R. P., et al. 1997, MNRAS, 285, L5

The End